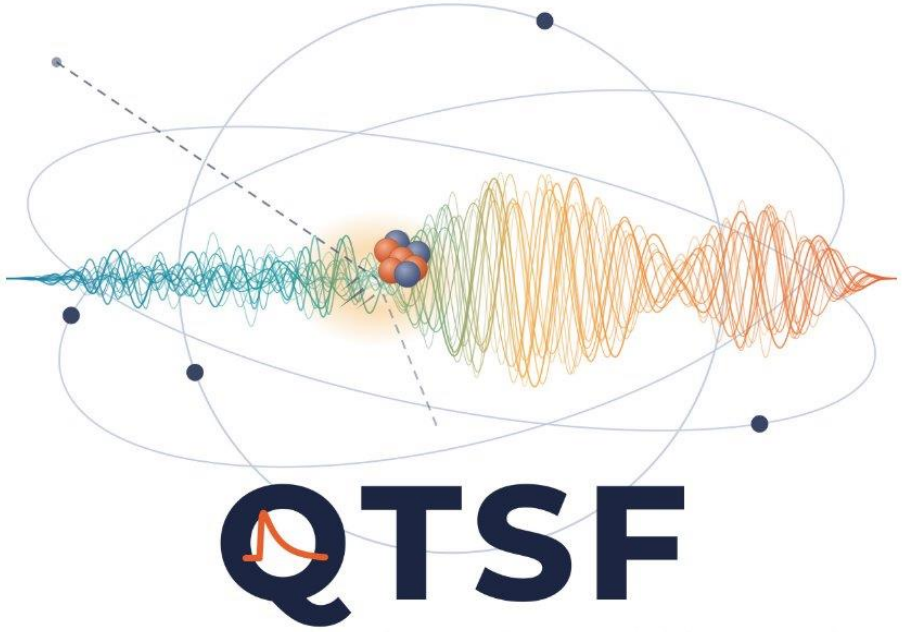
Characterizing Vibrations in a Dry Dilution Refrigerator for Low Noise Experiments

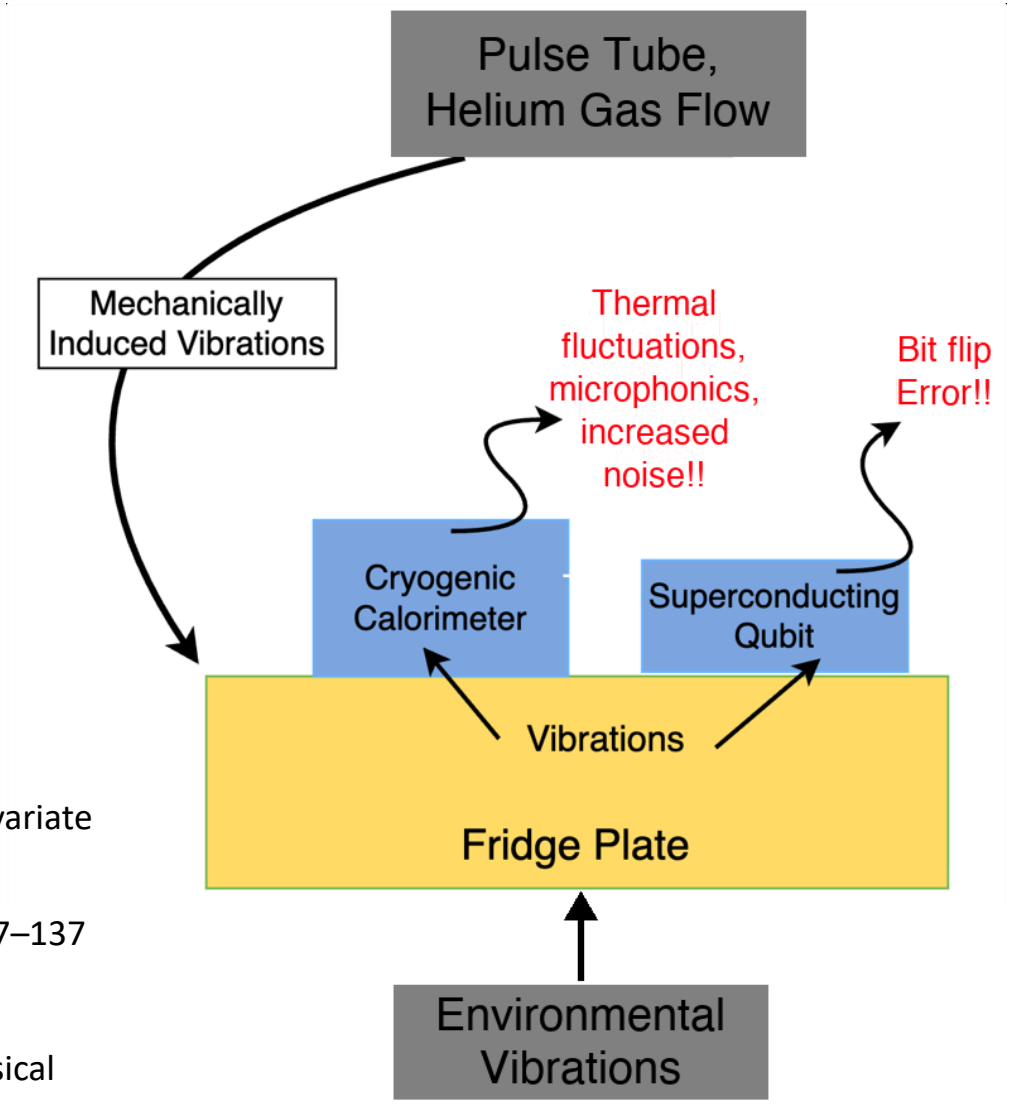
Jackson Fisher, Wouter Van De Pontseele, Lucia Steinke



Maybell

Importance of Vibrations

- Causes errors in superconducting qubits and degrades performance of sensitive particle detectors
- Affected experiments can include neutrino-nucleus scattering (RICOCHET), neutrinoless double beta-decay search (CUORE), dark matter search (SuperCDMS)...



K. J. Vetter et al., "Improving the performance of cryogenic calorimeters with nonlinear multivariate noise cancellation algorithms," The European Physical Journal C, vol. 84, no. 3, Mar. 2024.

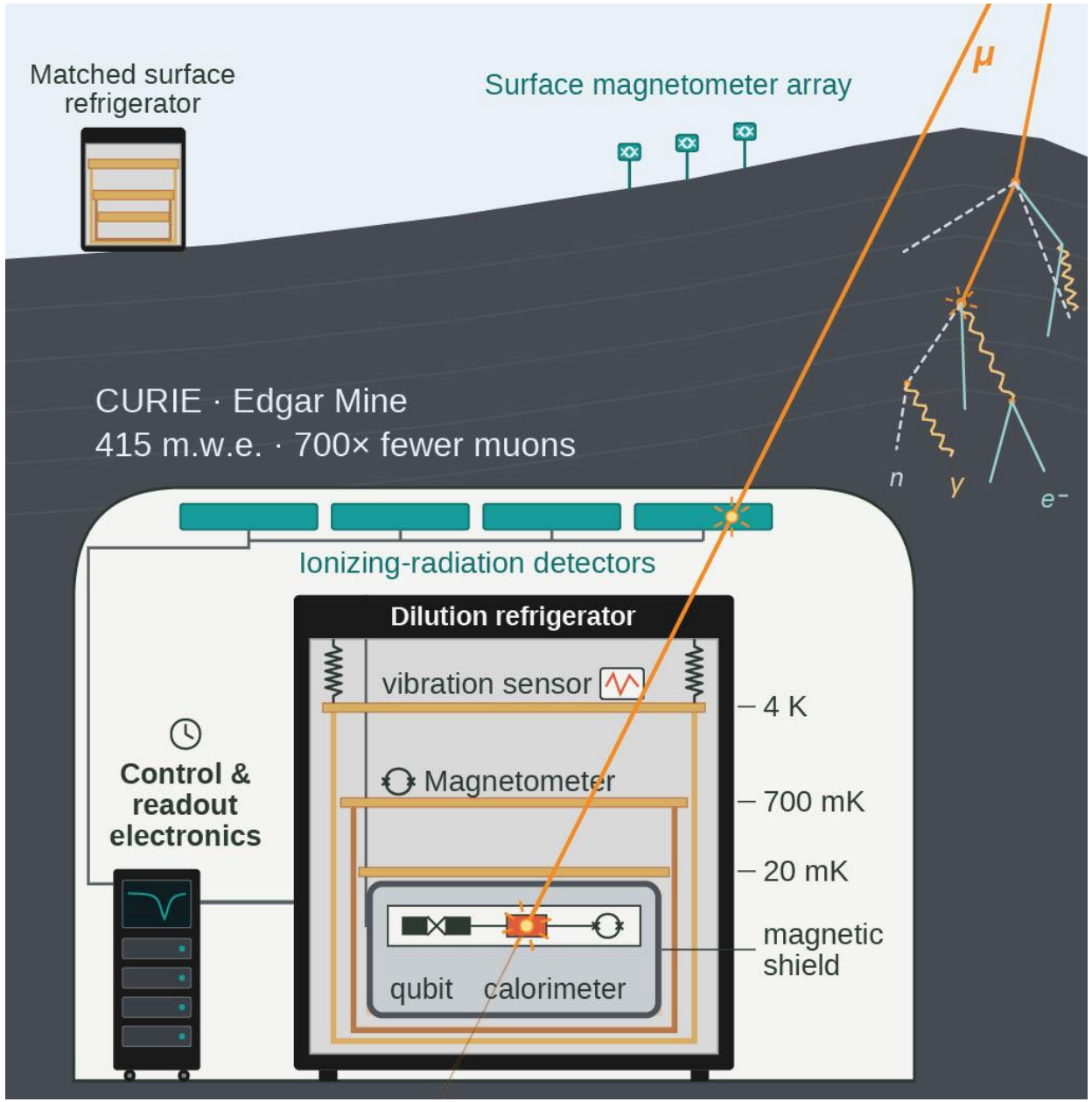
Augier, C., Beaulieu, G., Belov, V. et al. Ricochet Progress and Status. J Low Temp Phys 212, 127–137 (2023).

H. P. Binney et al., "Distinguishing Types of Correlated Errors in Superconducting Qubits," Physical Review Applied, vol. 26, no. 2, Art. no. 024025, Aug. 2026, doi: 10.1103/j235-47t6.

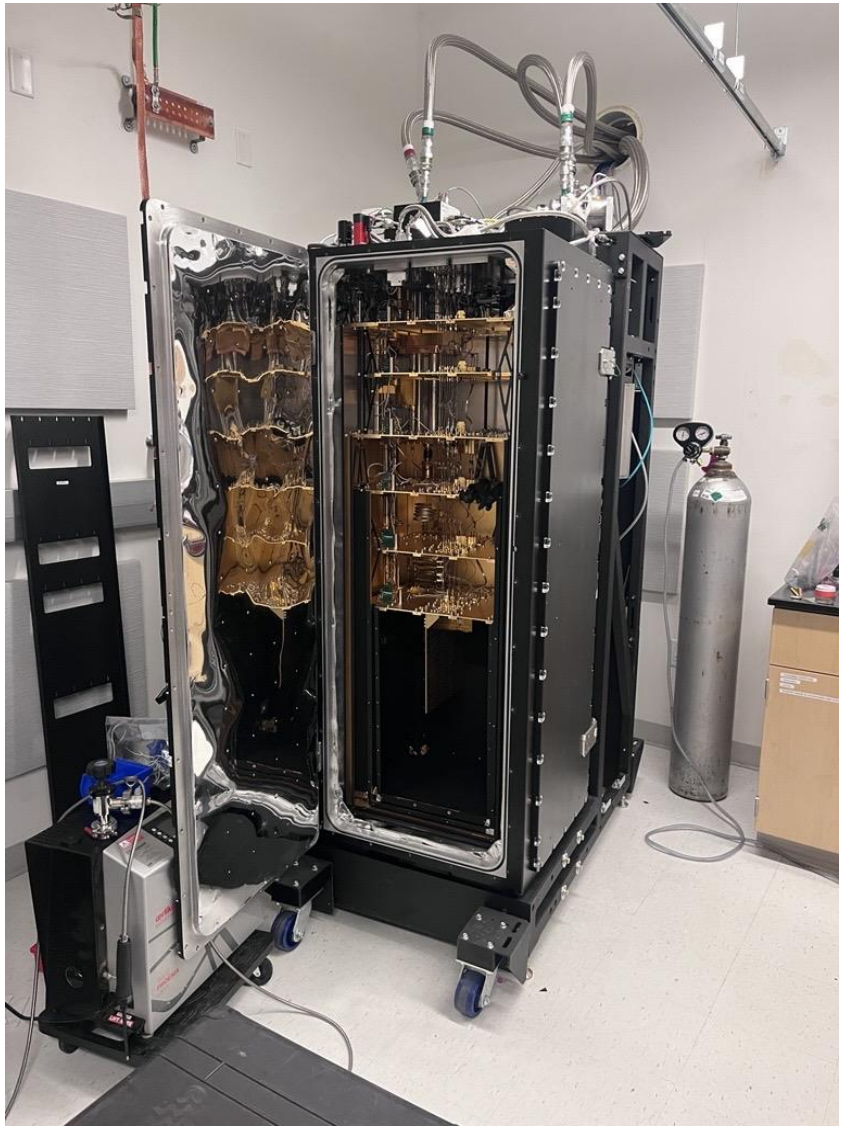
Colorado Underground Research Institute (CURIE)

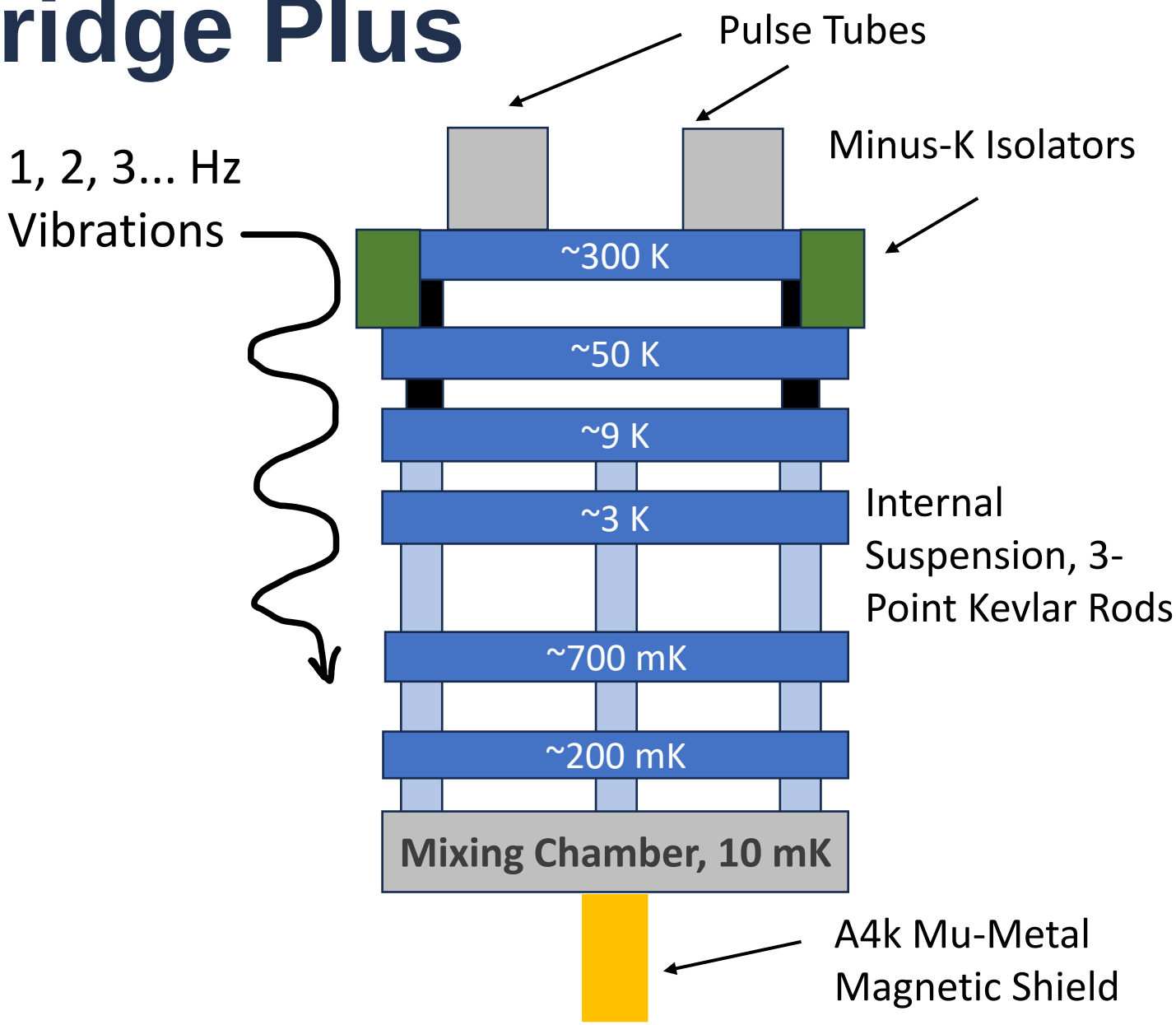
- Future physics lab located under ~200m of rock
- Measured 700x muon attenuation
- Vibrations, electromagnetic, and radon noise also important

Talk at CPAD: "The Colorado Underground Research Institute: Status and Site Characterization", Luke Wanner

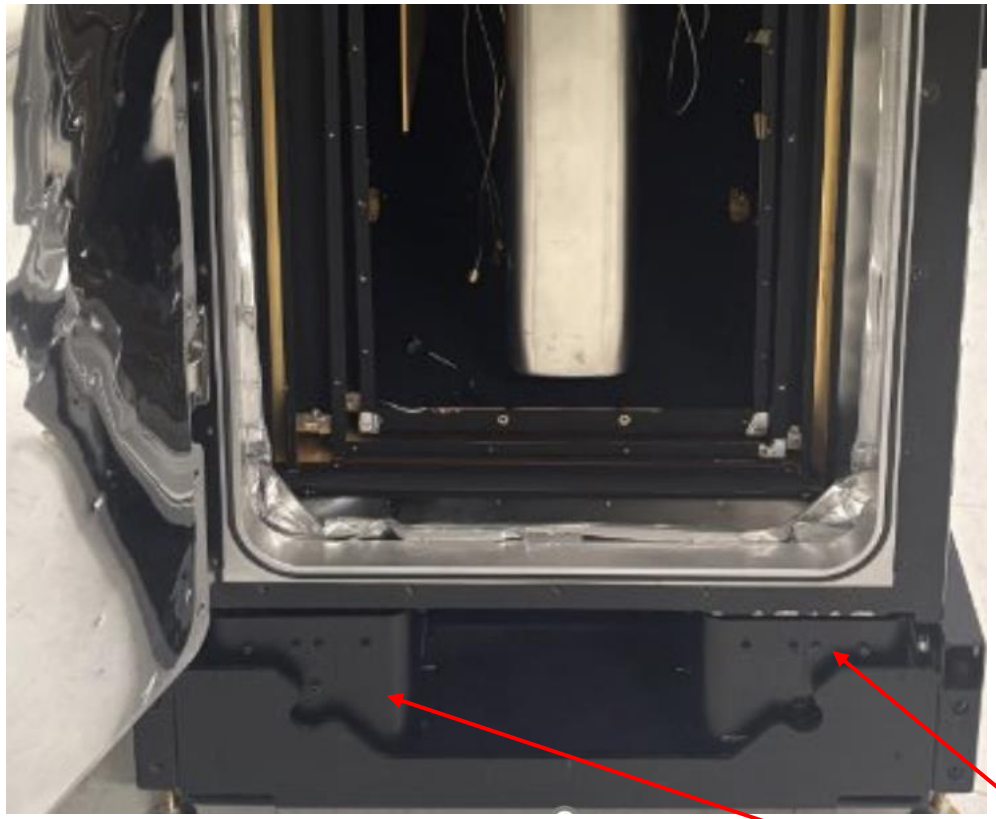


Maybell Quantum Fridge Plus

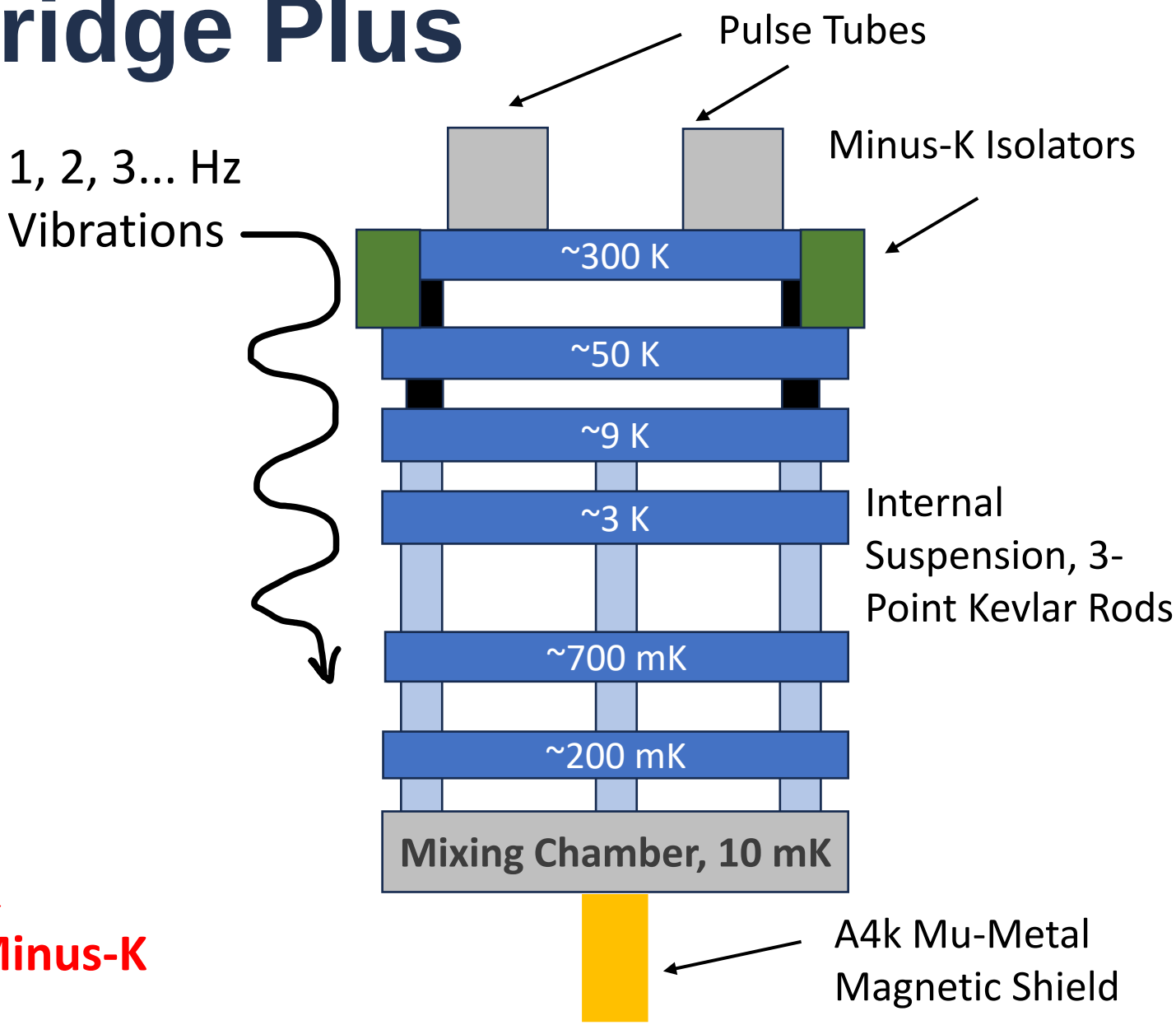




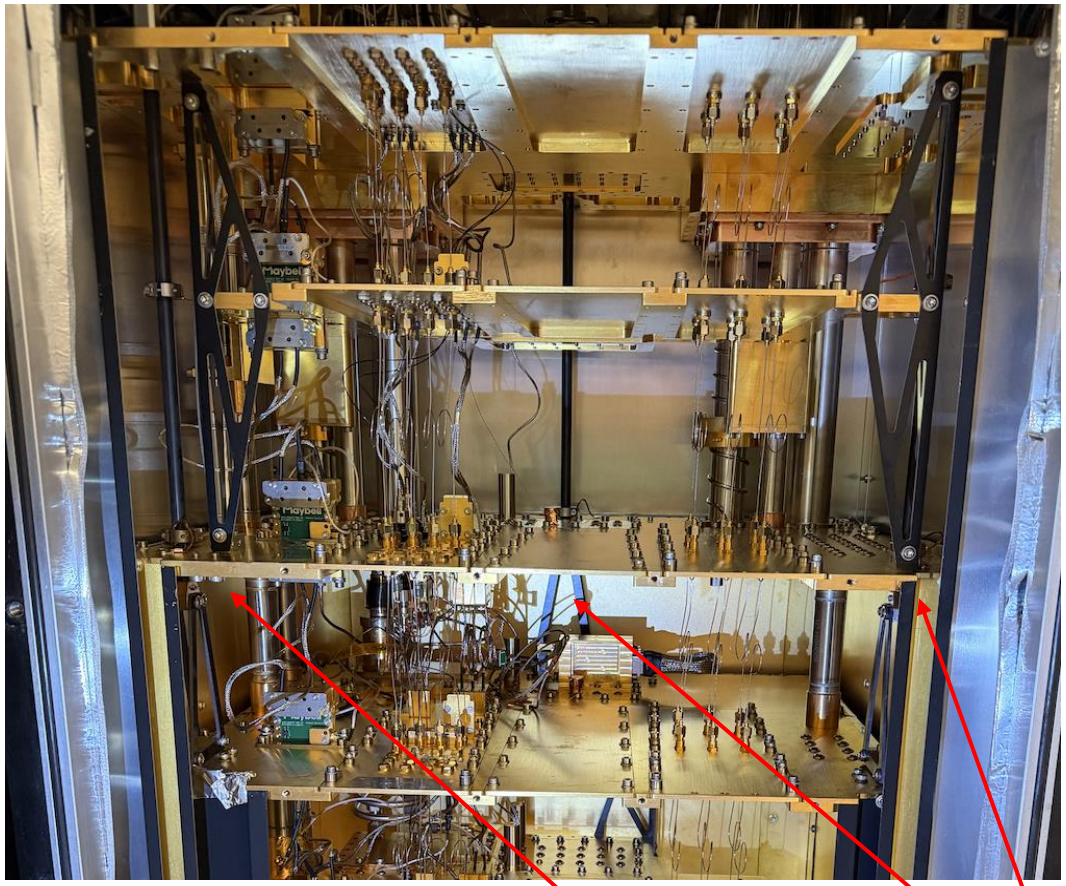
Maybell Quantum Fridge Plus



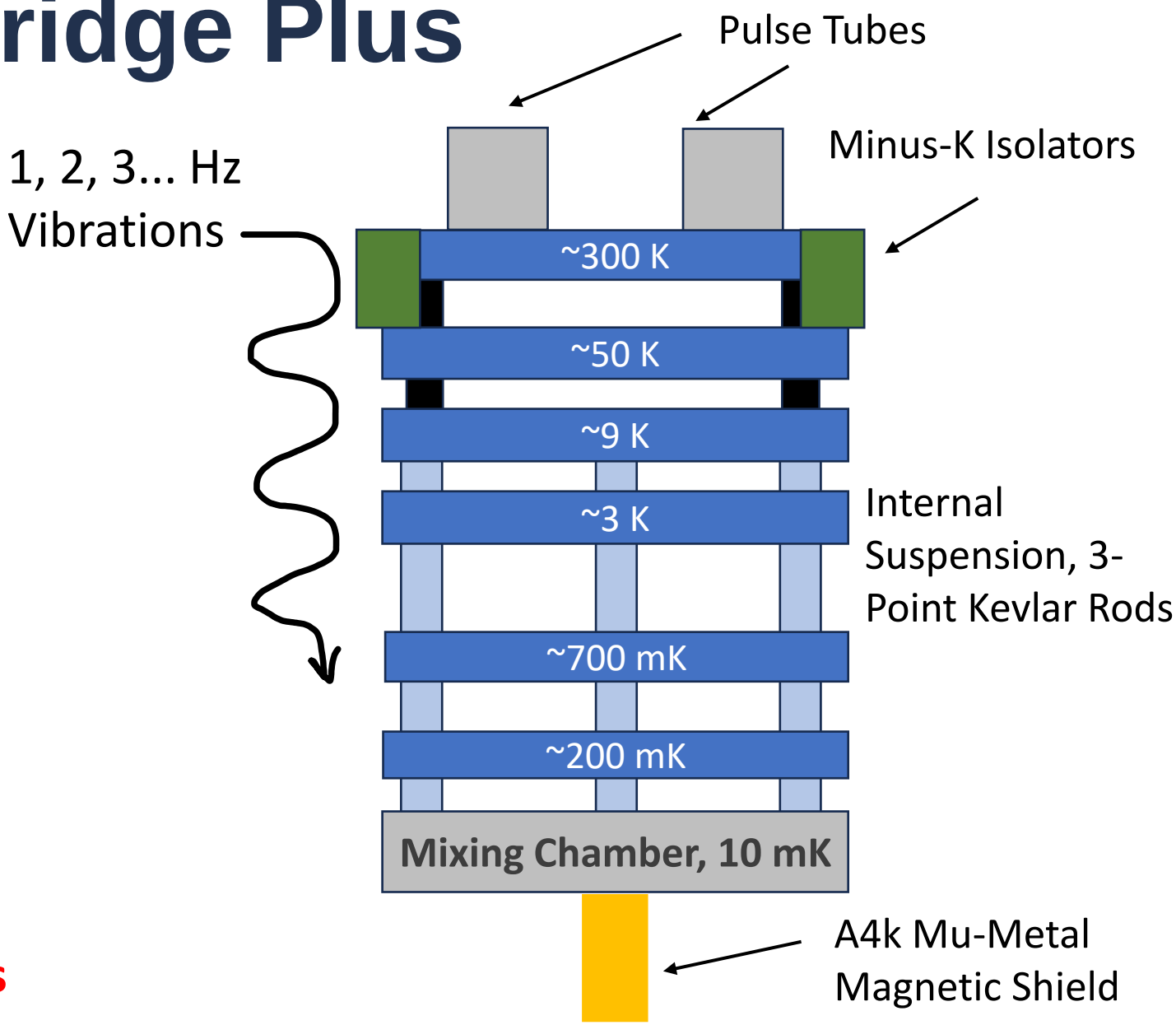
Minus-K



Maybell Quantum Fridge Plus



Kevlar Rods



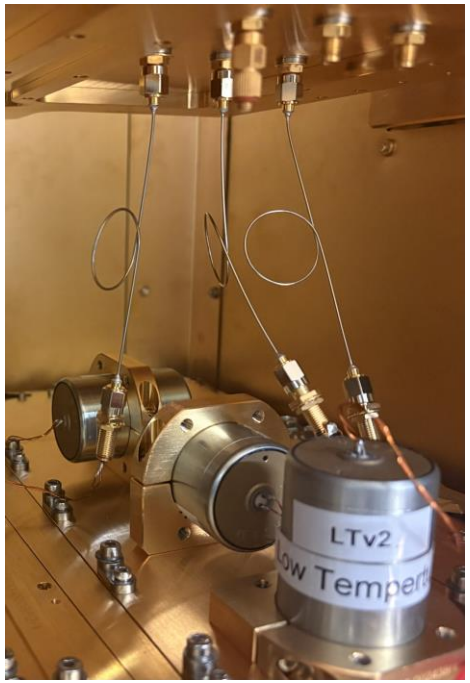
Piezoelectric Sensors and Geophones



2271A (Lowtemp)
PCB Piezotronics



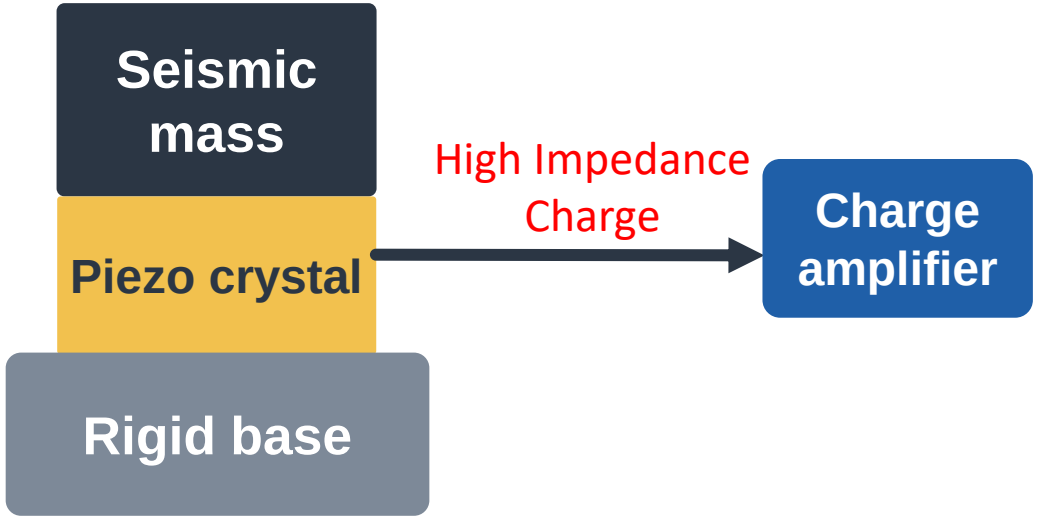
393B05 (Roomtemp)
PCB Piezotronics



HG-2 Geophones
HGS Products

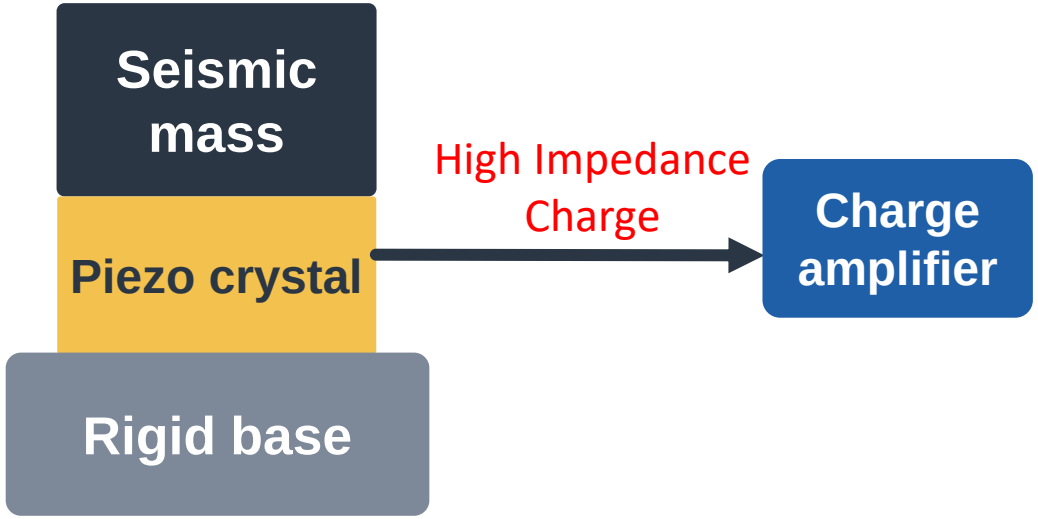
Sensor Operation and Specifications

Piezoelectric

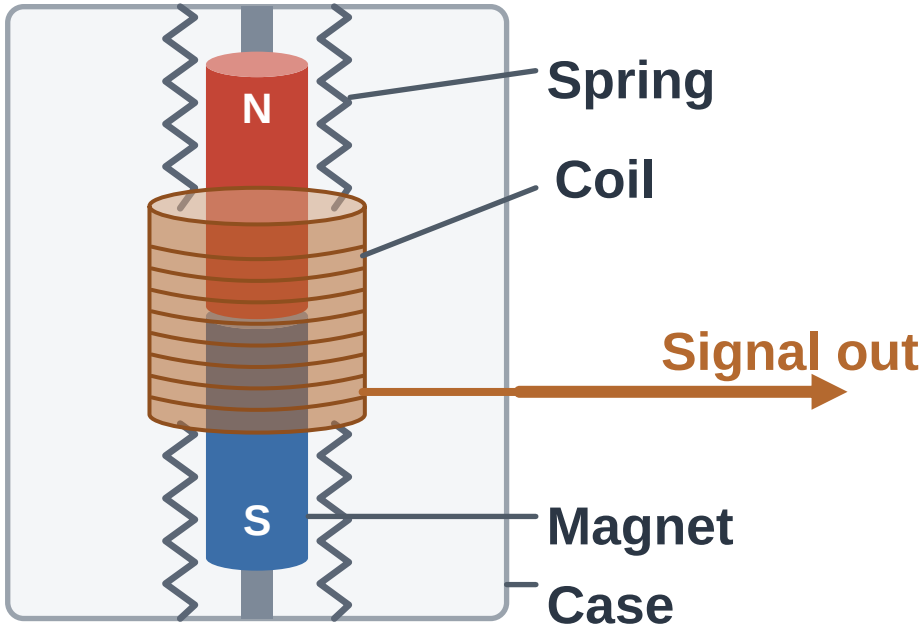


Sensor Operation and Specifications

Piezoelectric

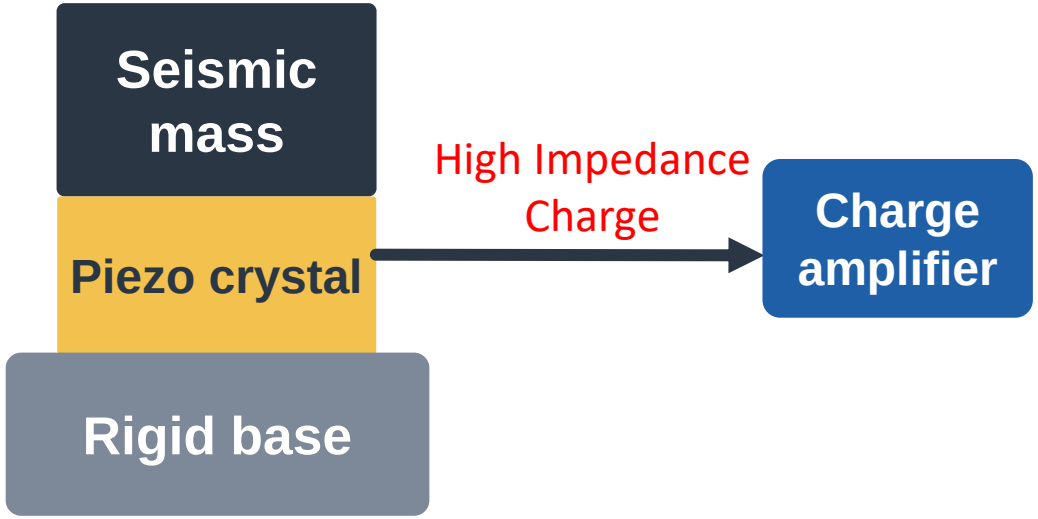


Geophone

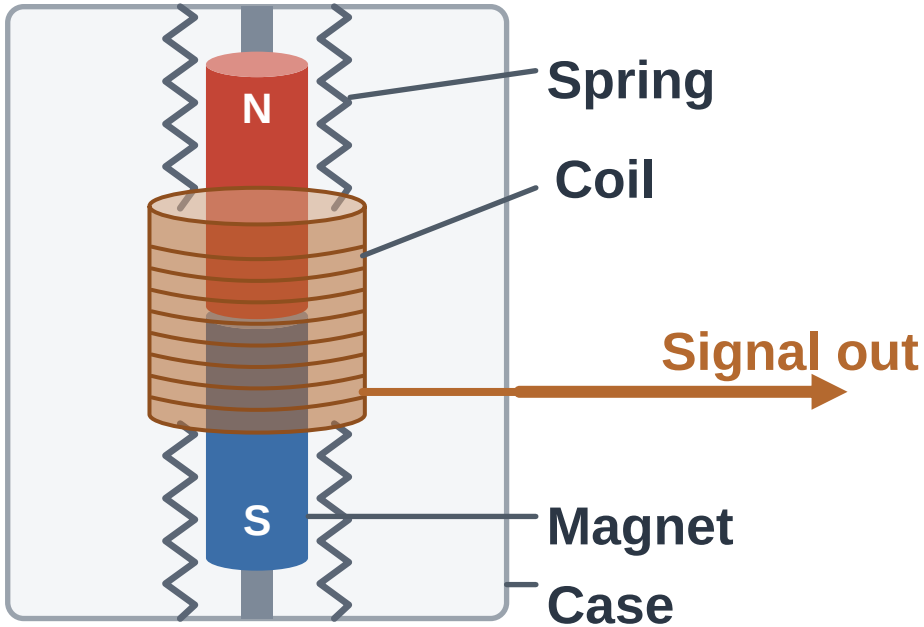


Sensor Operation and Specifications

Piezoelectric

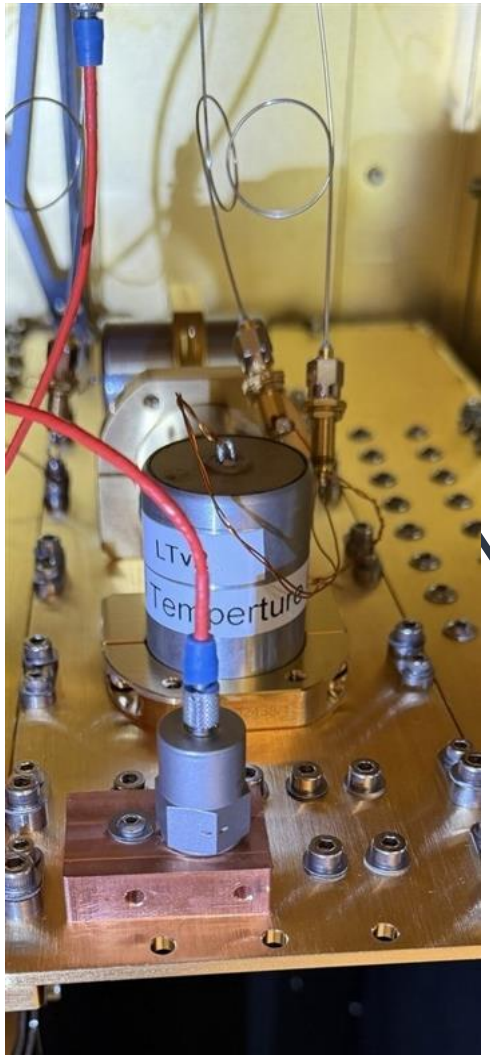


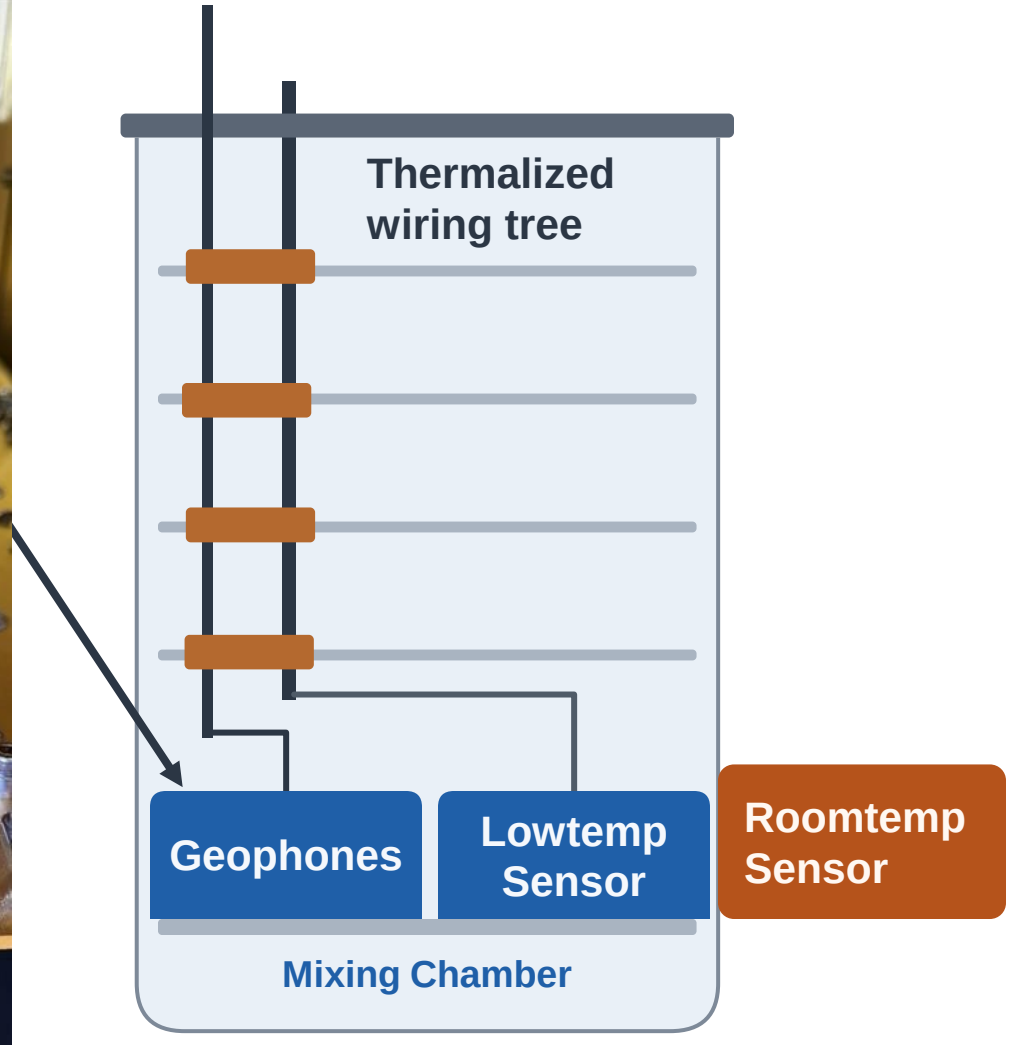
Geophone



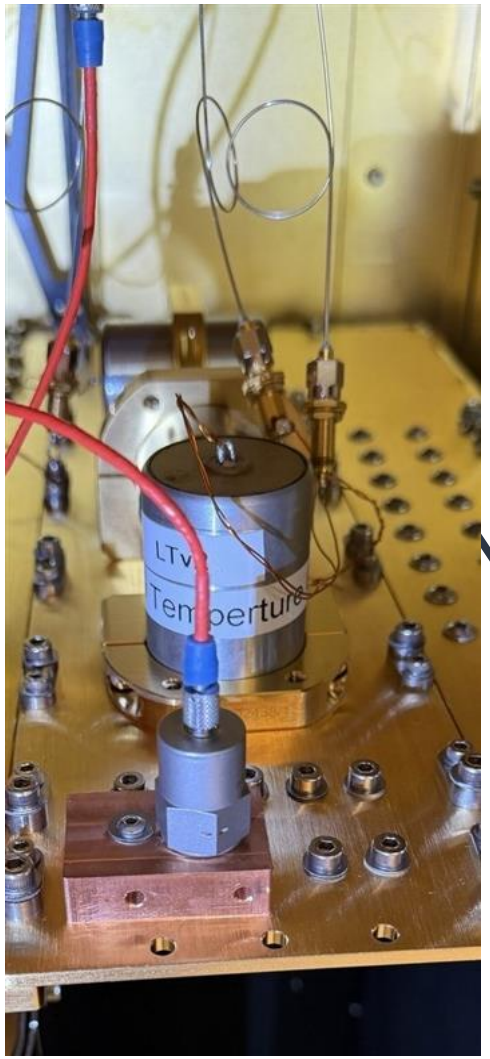
Sensor	Lowtemp	Roomtemp	Geophone
Frequency Range	DC to 4 kHz	DC to 500 Hz	DC to 100 Hz
Sensitivity Deviation due to Temperature	-15 % at ~5 K	Not cryo-compatible	Unknown

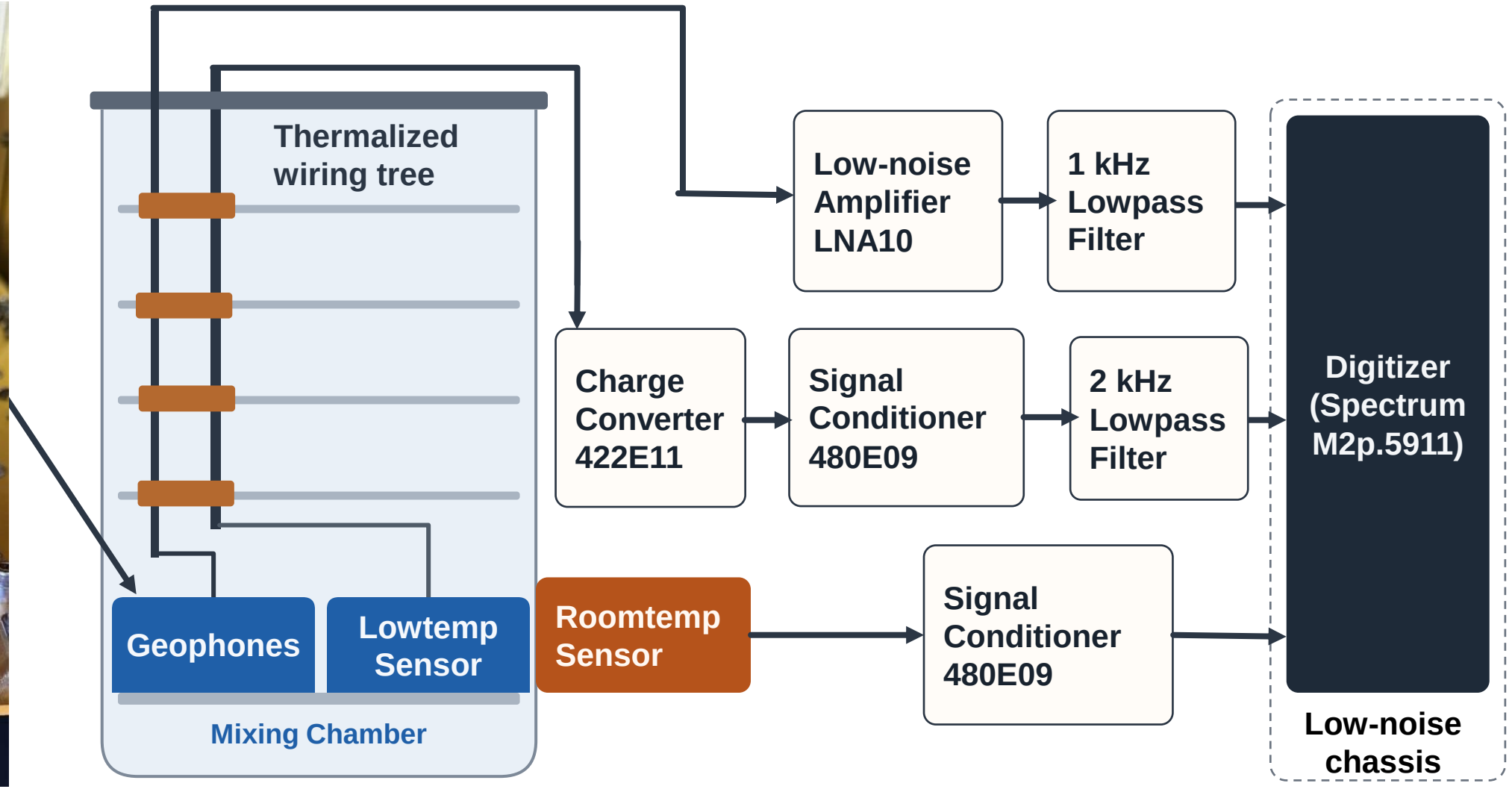
Accelerometer Measurement Chain





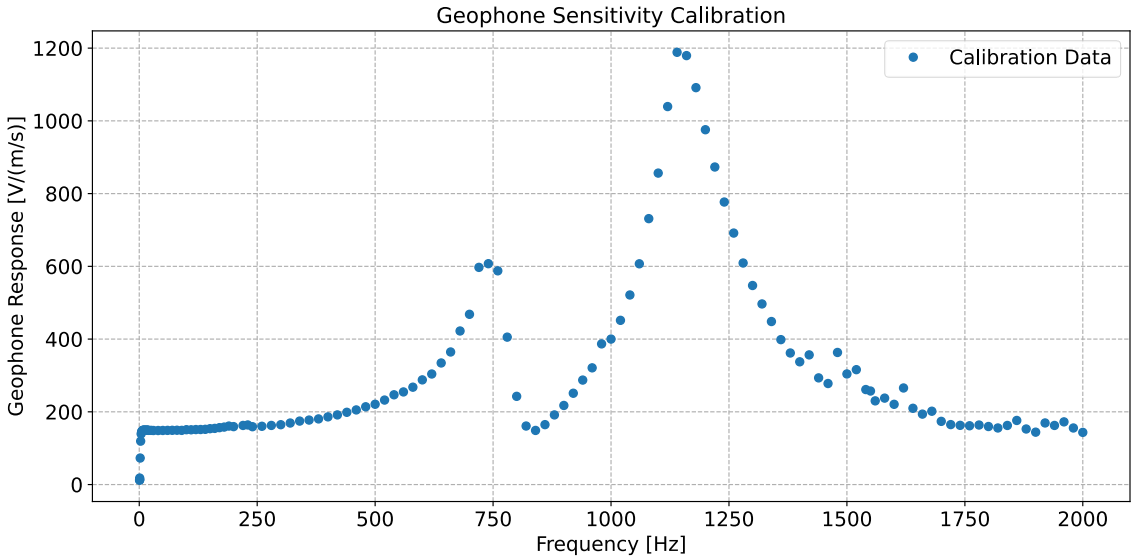
Accelerometer Measurement Chain





Data Analysis

Sensor Calibration



Lowtemp Flat Sensitivity: 0.1249 V / (m/s^2)

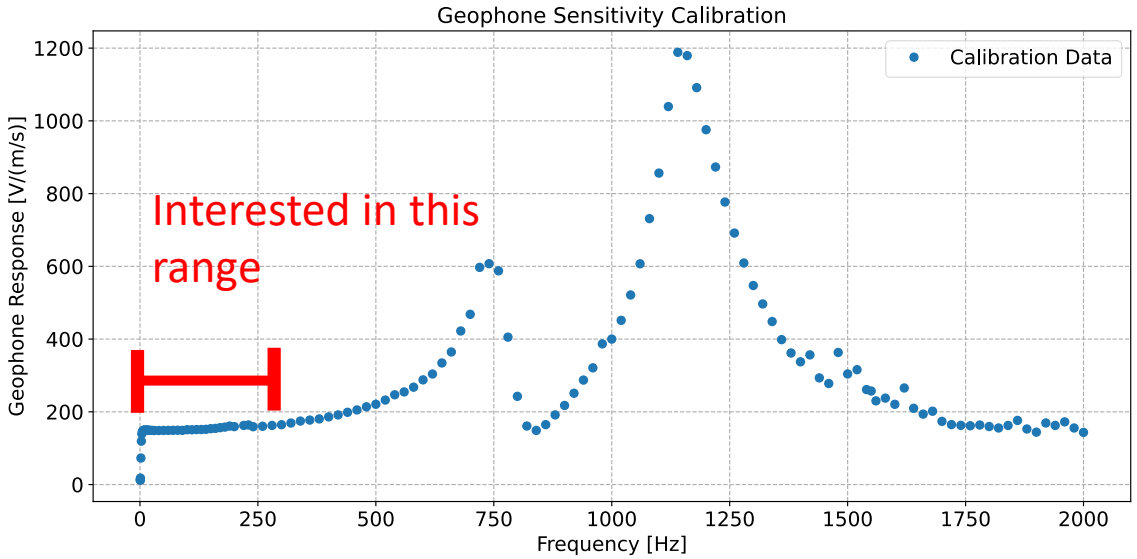
Roomtemp Flat Sensitivity: 1.042 V / (m/s^2)

Amplitude Spectral Density (Welch's Method)

RMS Displacement

Data Analysis

Sensor Calibration



Lowtemp Flat Sensitivity: 0.1249 V / (m/s^2)

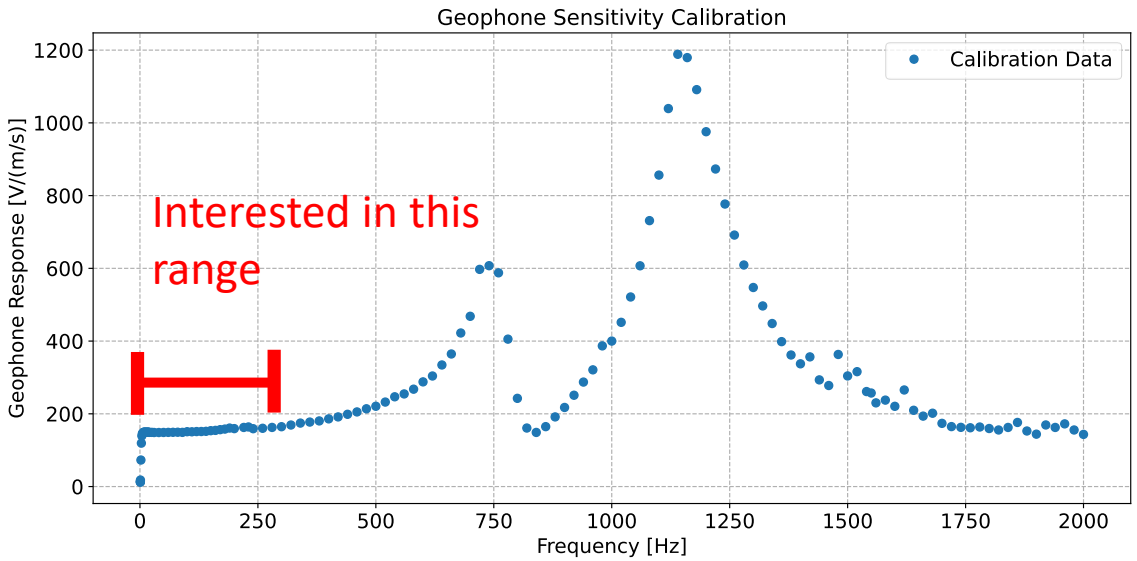
Roomtemp Flat Sensitivity: 1.042 V / (m/s^2)

Amplitude Spectral Density (Welch's Method)

RMS Displacement

Data Analysis

Sensor Calibration



Lowtemp Flat Sensitivity: 0.1249 V / (m/s^2)

Roomtemp Flat Sensitivity: 1.042 V / (m/s^2)

Amplitude Spectral Density (Welch's Method)

1. Average FFTs, apply Hanning windowing (U)

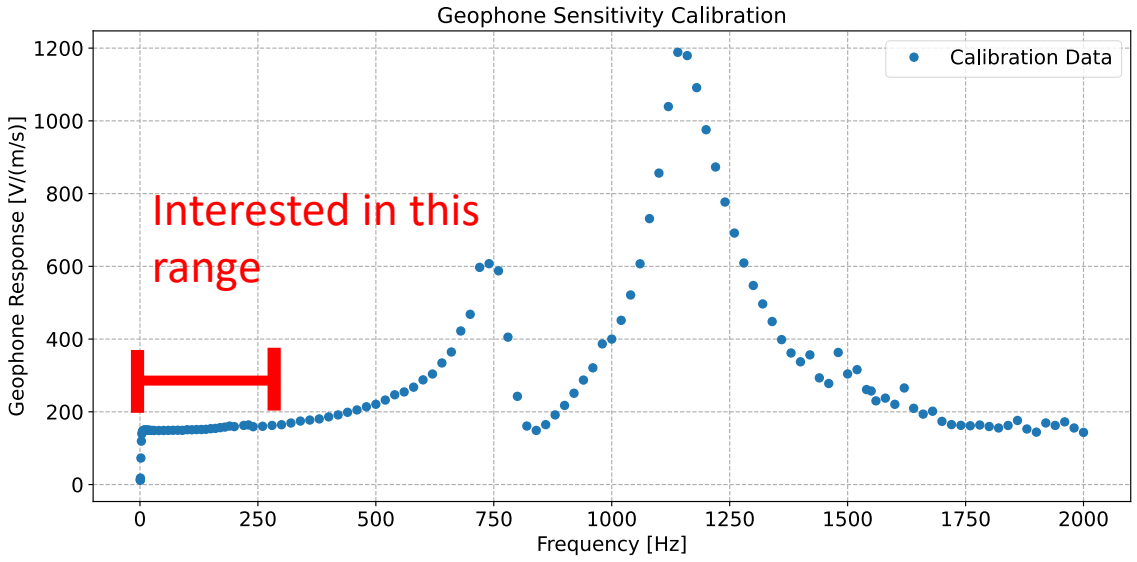
$$\mathrm{PSD}(f_i) = \frac{2}{f_s U}\frac{1}{K}\sum_{k=0}^{K-1} X_k^*(f_i)\, X_k(f_i)$$

2. Calculate ASD $\quad \mathrm{ASD}(f_i) = \sqrt{\mathrm{PSD}(f_i)}$

RMS Displacement

Data Analysis

Sensor Calibration



Lowtemp Flat Sensitivity: 0.1249 V / (m/s^2)

Roomtemp Flat Sensitivity: 1.042 V / (m/s^2)

Amplitude Spectral Density (Welch's Method)

1. Average FFTs, apply Hanning windowing (U)

$$\mathrm{PSD}(f_i) = \frac{2}{f_s U}\frac{1}{K}\sum_{k=0}^{K-1} X_k^*(f_i)\, X_k(f_i)$$

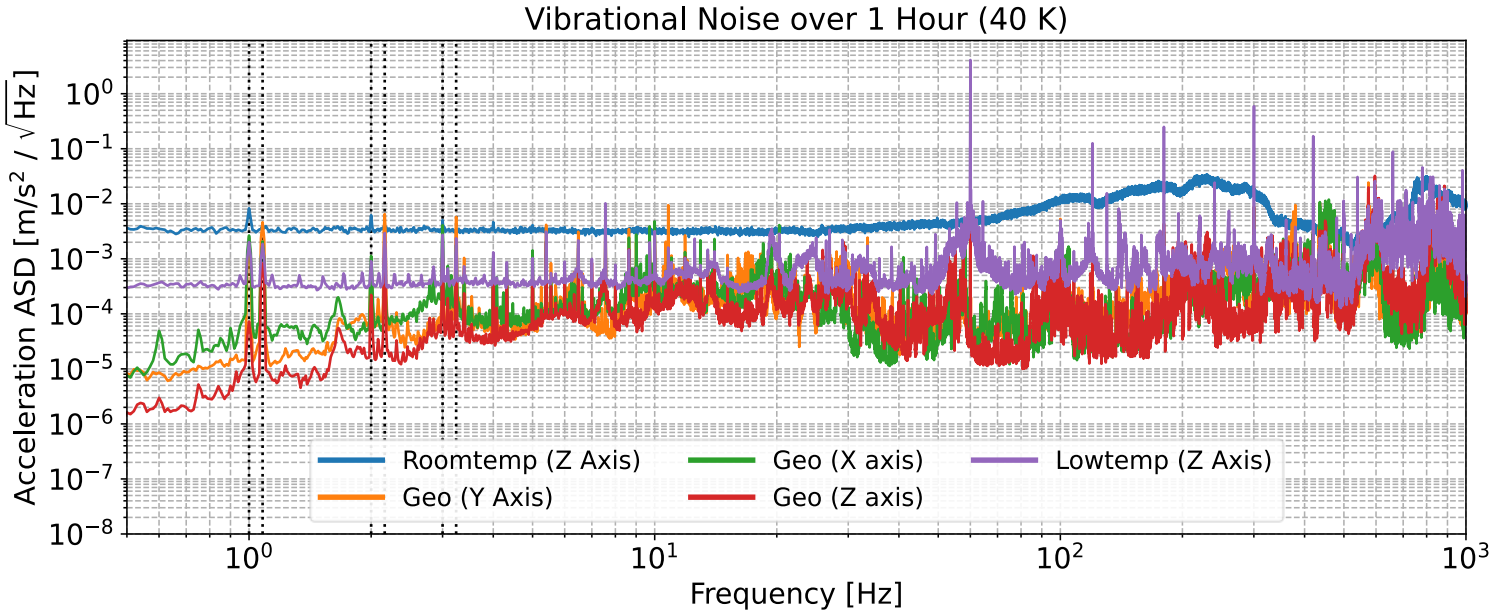
2. Calculate ASD $\quad \mathrm{ASD}(f_i) = \sqrt{\mathrm{PSD}(f_i)}$

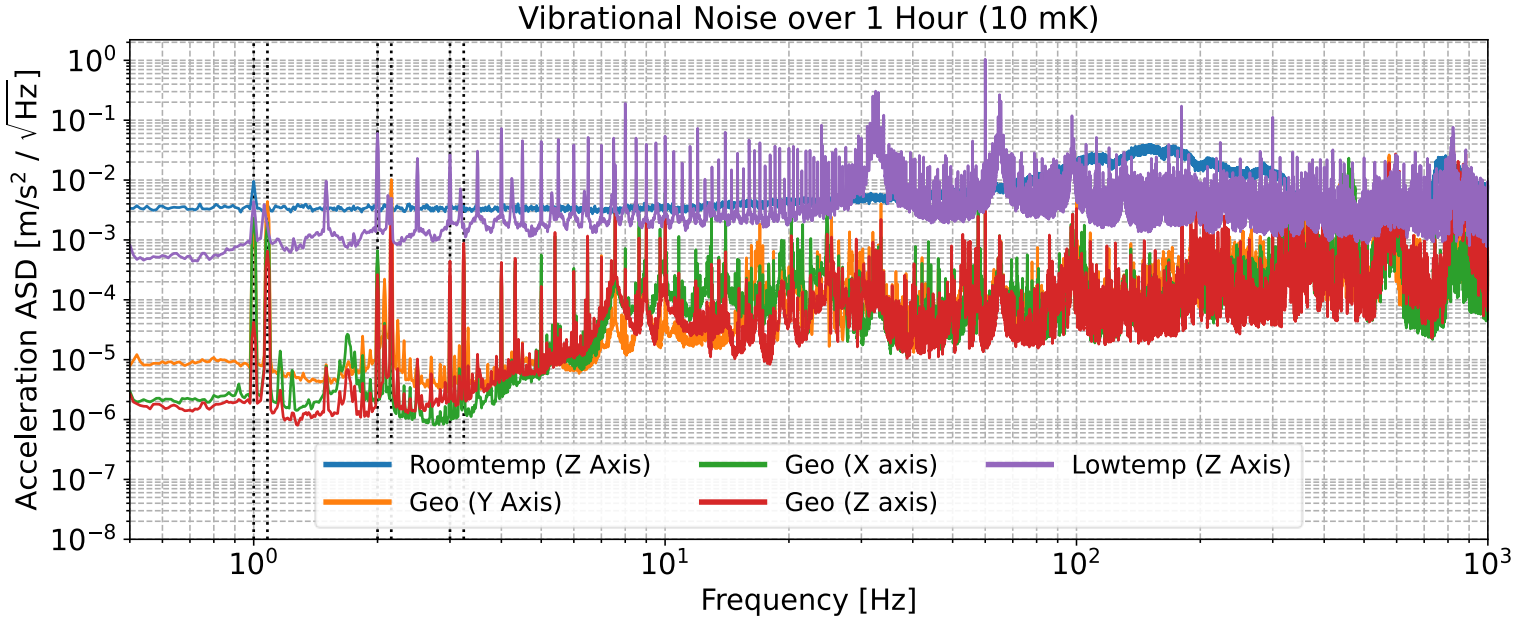
RMS Displacement

3. Calculate Displacement ASD $\quad \mathrm{ASD}_d(f_i) = \frac{\mathrm{ASD}_a(f_i)}{(2\pi f_i)^2}$

4. Calculate RMS Displacement $\quad d_{\mathrm{rms}} = \sqrt{\sum_{i=1}^{L/2} \mathrm{ASD}_d(f_i)^2\, \Delta f}$

Low Temperature Measurement





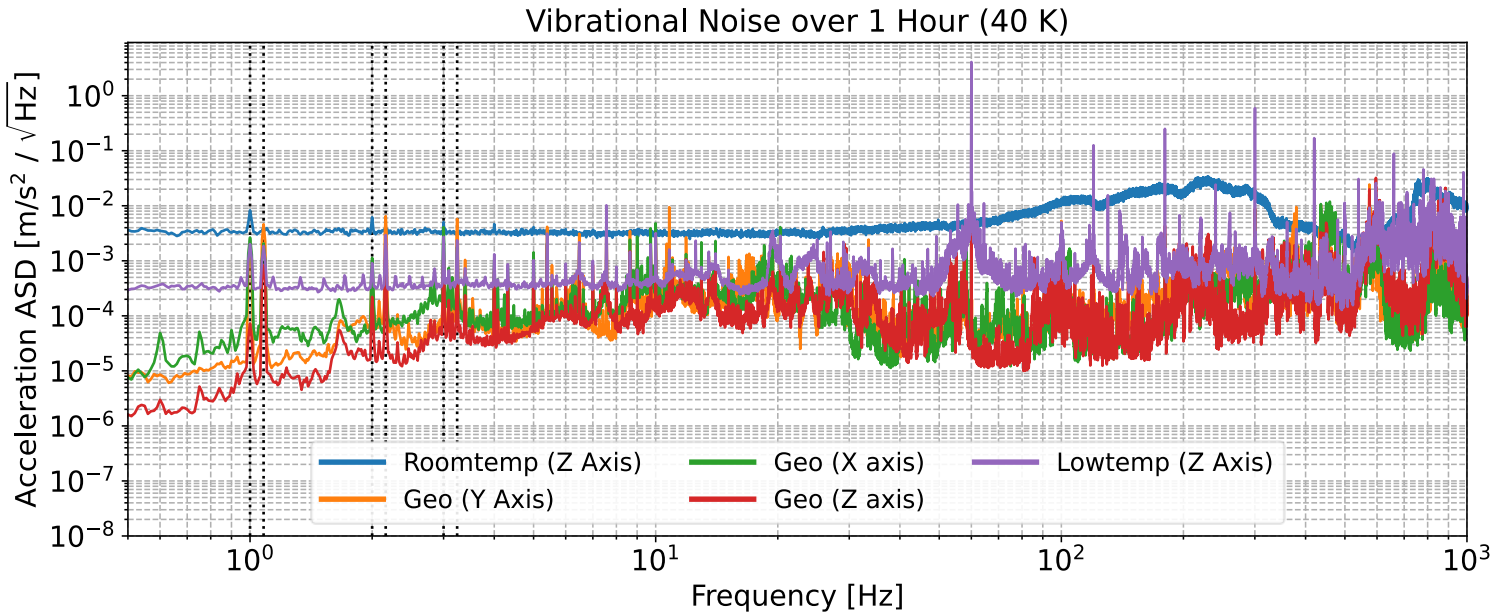
Low Temperature Measurement

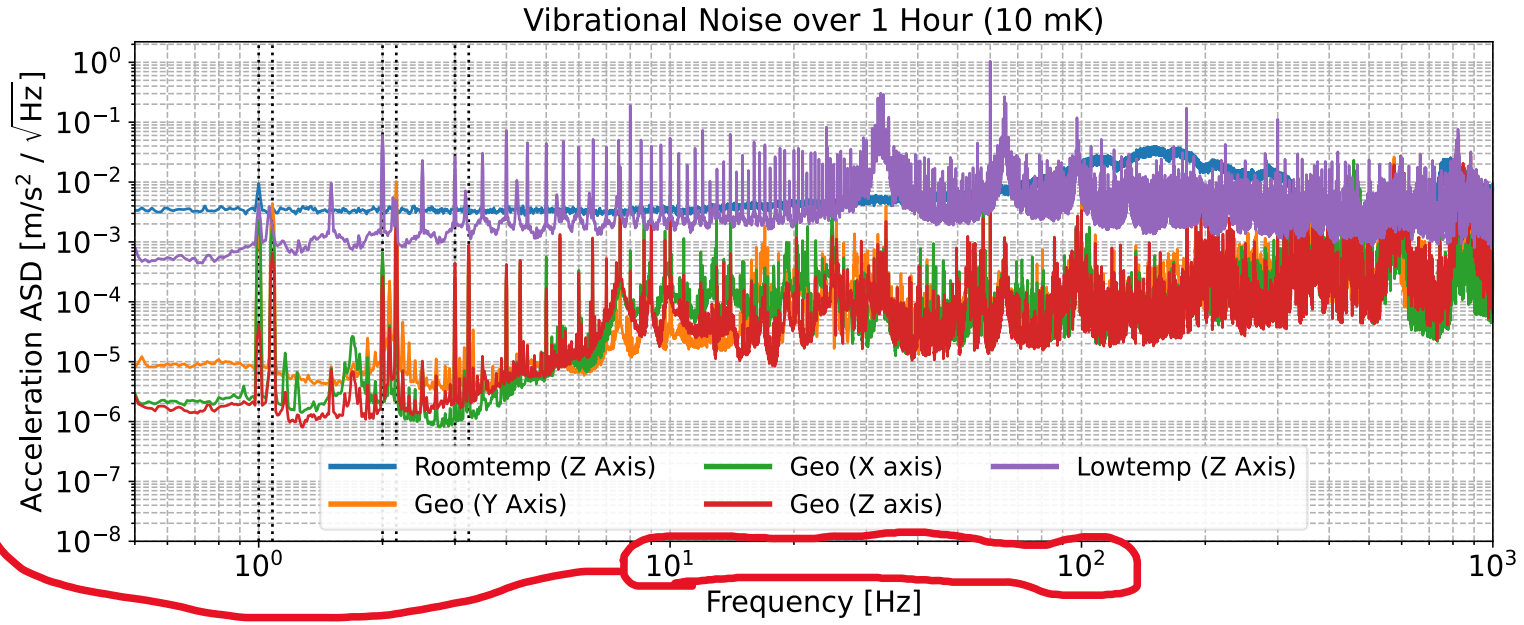
From Geophones, RMS displacement from 10 Hz to 200 Hz:

Z Axis = 86.7 nm

X Axis = 209.4 nm

Y Axis = 70.2 nm





Low Temperature Measurement

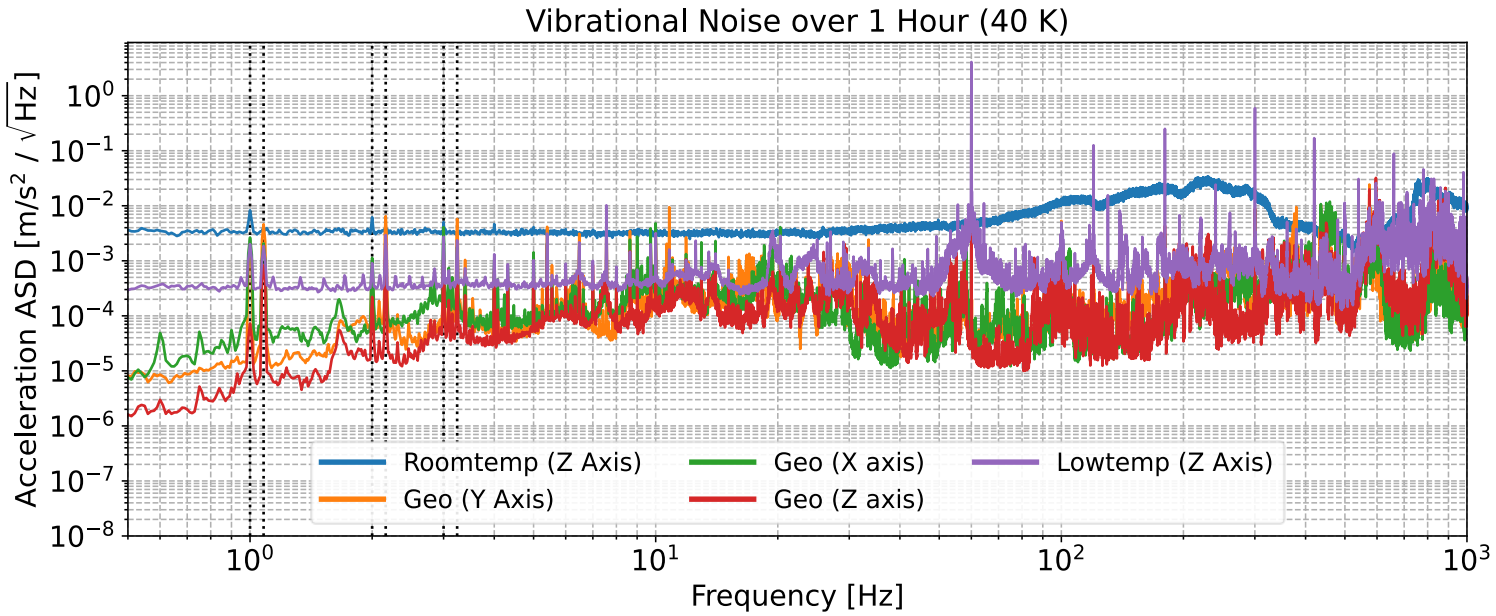
Calibration at cryogenic temperature not confirmed

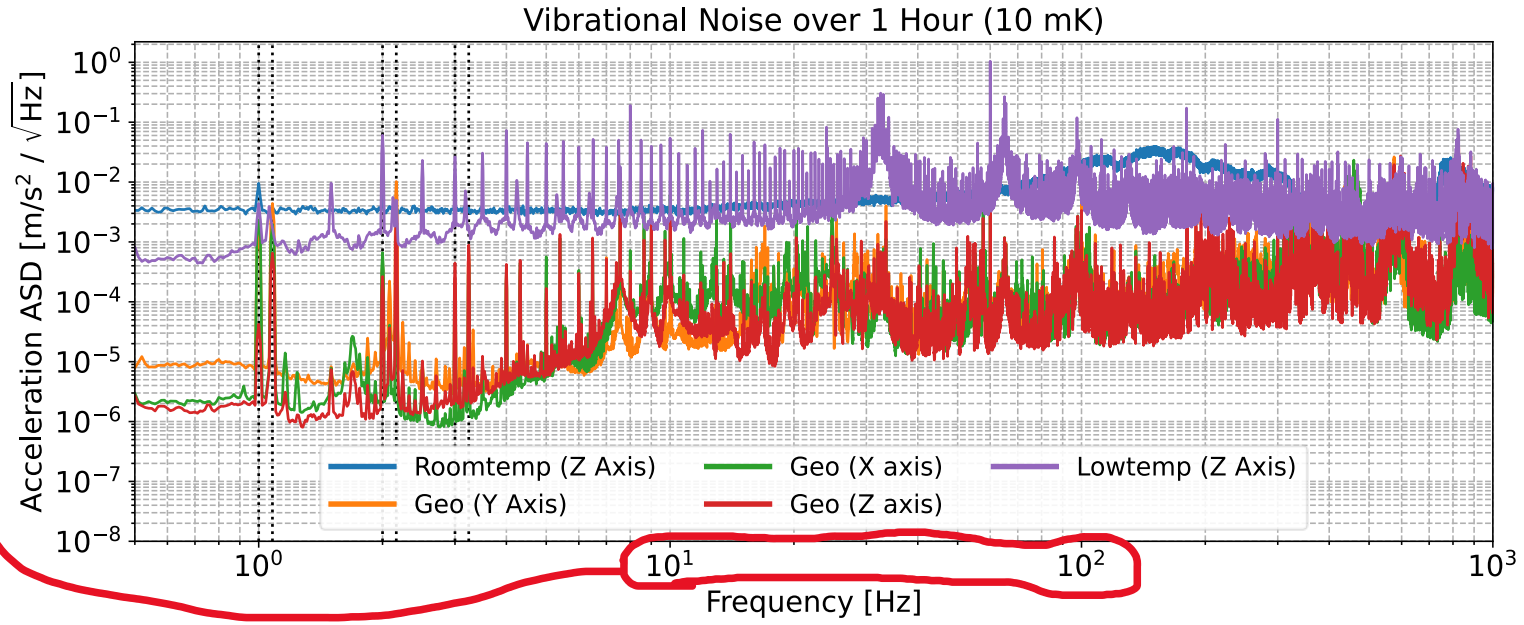
From Geophones, RMS displacement from 10 Hz to 200 Hz:

Z Axis = 86.7 nm

X Axis = 209.4 nm

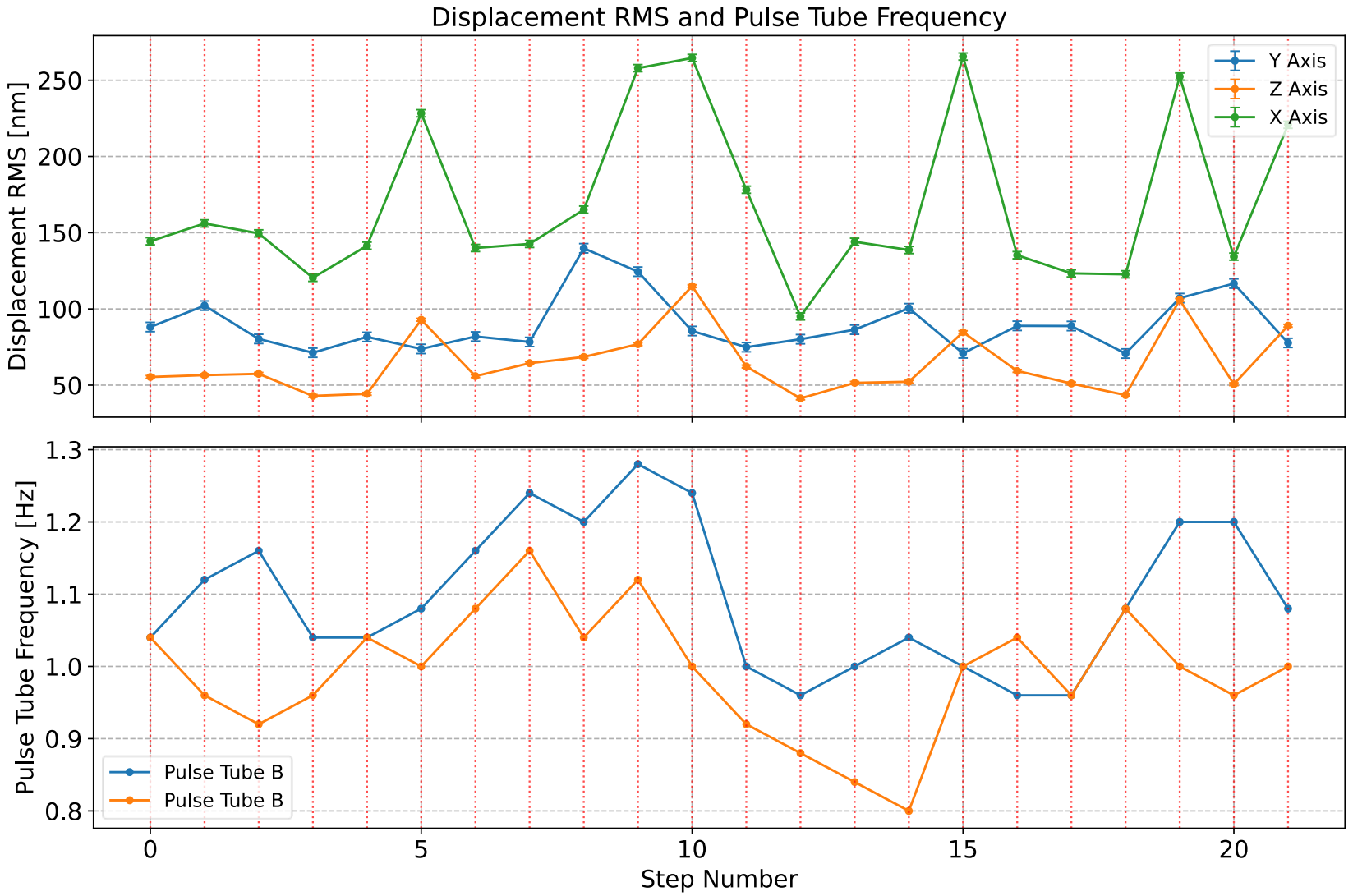
Y Axis = 70.2 nm



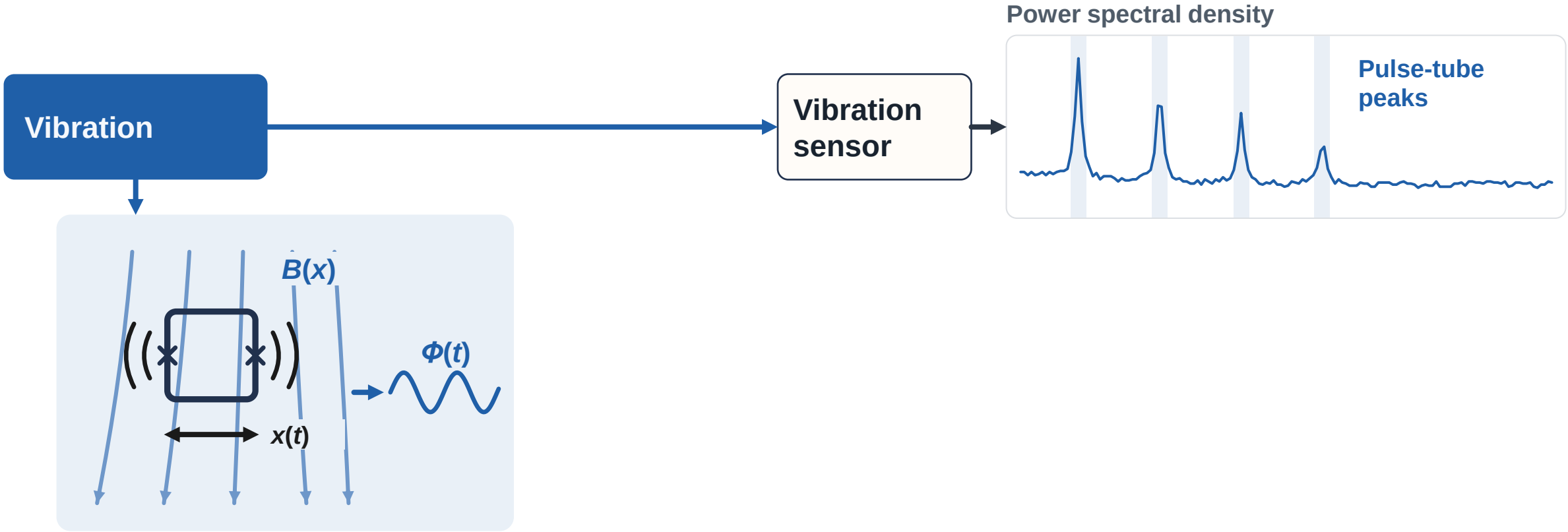


Noise Correlation

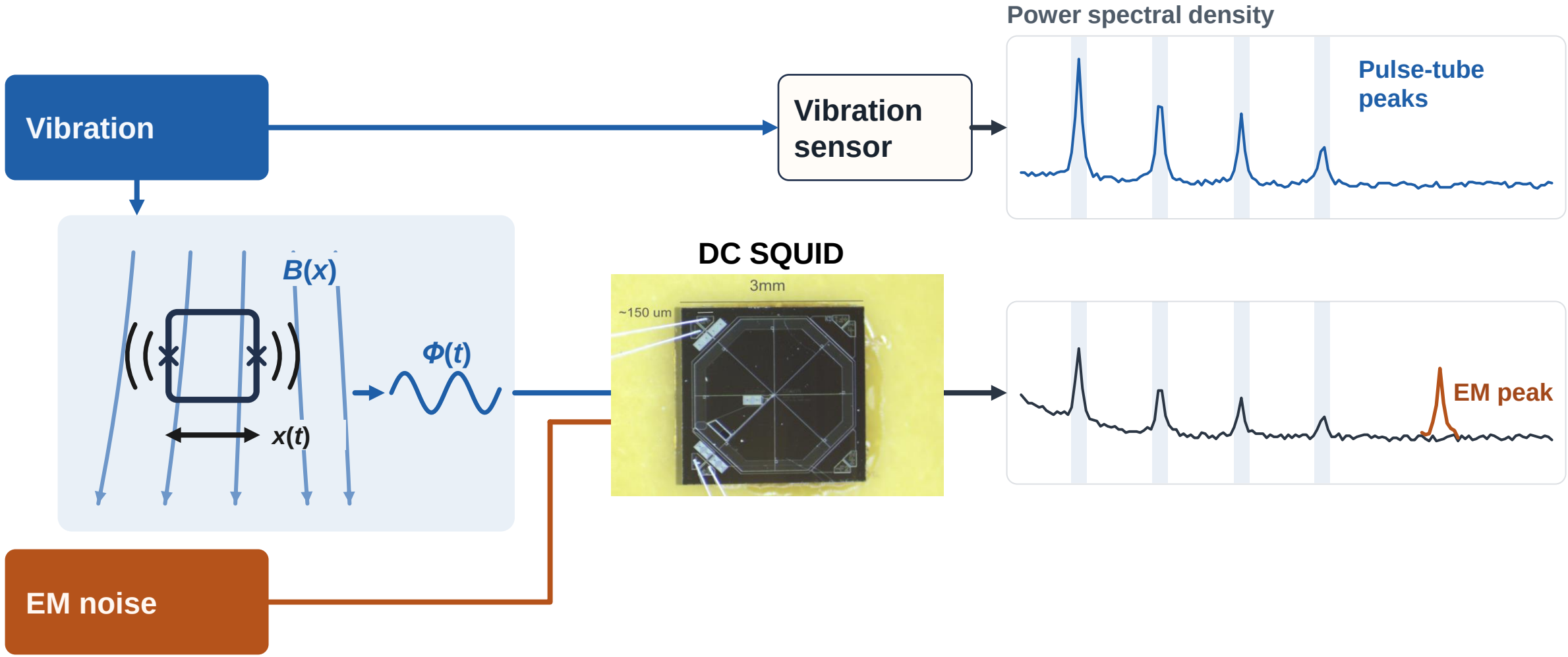
- Exploring further vibration mitigation
- Finding optimal compressor frequency combination for vibration and cooling power
- Other tests can include tuning Minus-K, decoupling rotary valves, positional measurement



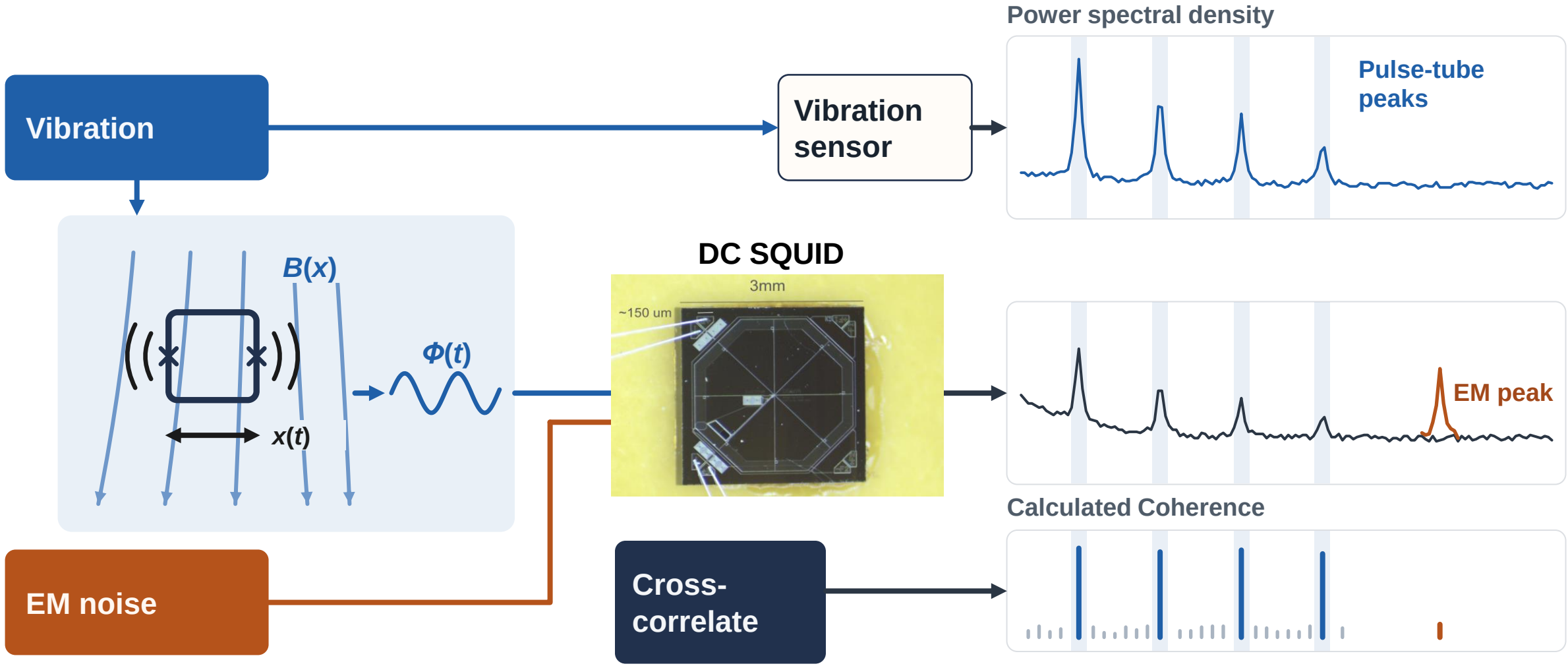
SQUID Cross Correlation



SQUID Cross Correlation



SQUID Cross Correlation

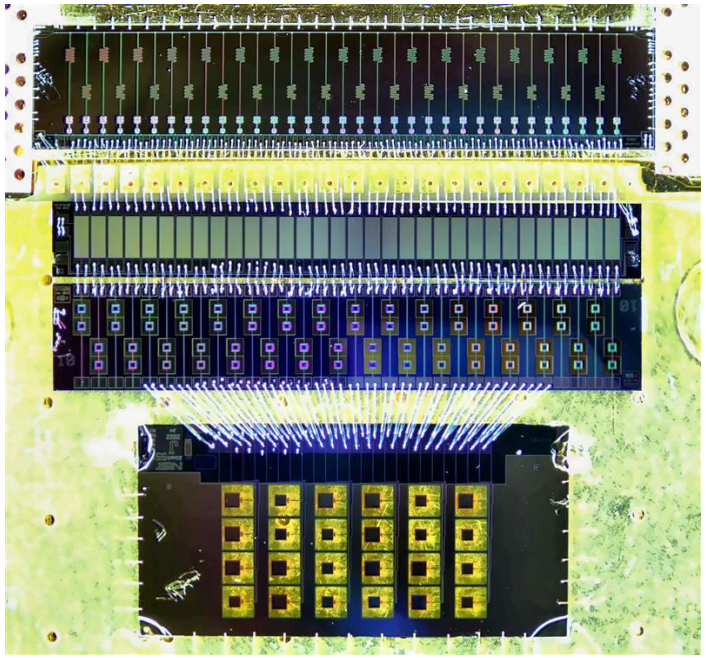


Conclusions

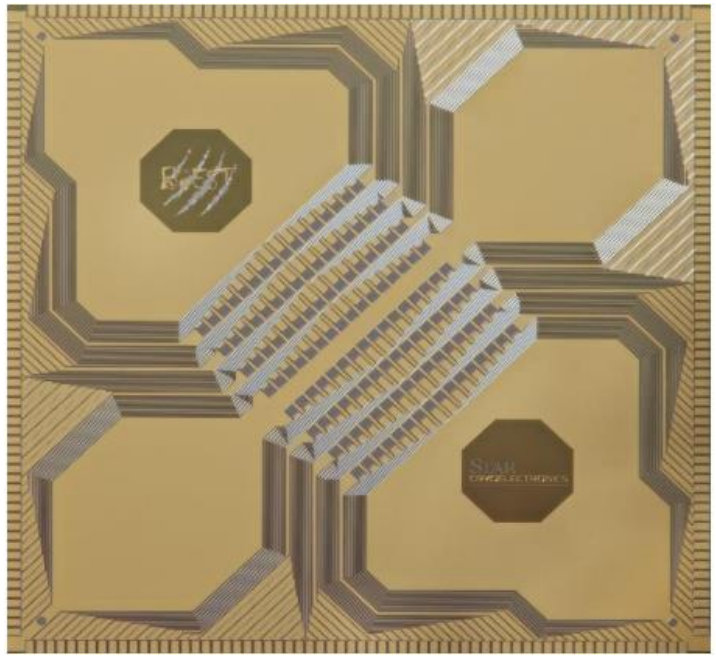
- Functional sensor setup, **looking for ideas to improve calibration and sensor noise**

- **Cross-correlation functions** with SQUID magnetometer, transition edge sensors (TES), superconducting tunnel junctions (STJ), superconducting qubits to identify and mitigate noise

TES Picture



STJ Picture



Bi-Weekly vibrational noise meetings:

THE BeEST

Acknowledgements

Maybell

QTSF

Quantum Technologies at the Sensitivity Frontier



jtfisher@mines.edu

https://qtsf.mines.edu/

Vibrational noise meeting Interest:

References

[1] K. J. Vetter et al., “Improving the performance of cryogenic calorimeters with nonlinear multivariate noise cancellation algorithms,” The European Physical Journal C, vol. 84, no. 3, Mar. 2024. doi:10.1140/epjc/s10052-024-12595-y

[2] Augier, C., Beaulieu, G., Belov, V. et al. Ricochet Progress and Status. J Low Temp Phys 212, 127–137 (2023). https://doi.org/10.1007/s10909-023-02971-5

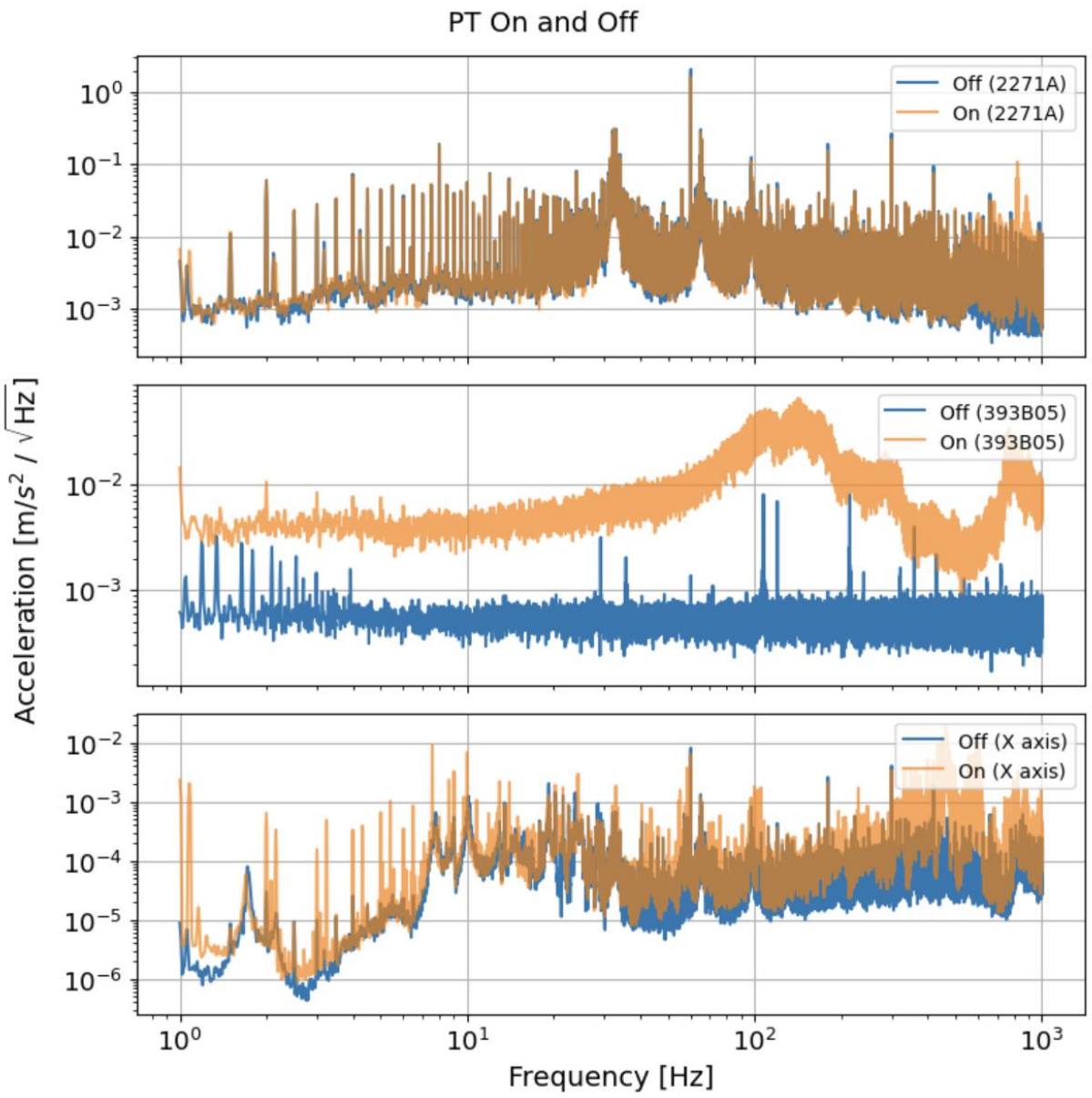
[3] H. P. Binney et al., “Distinguishing Types of Correlated Errors in Superconducting Qubits,” Physical Review Applied, vol. 26, no. 2, Art. no. 024025, Aug. 2026, doi: 10.1103/j235-47t6.

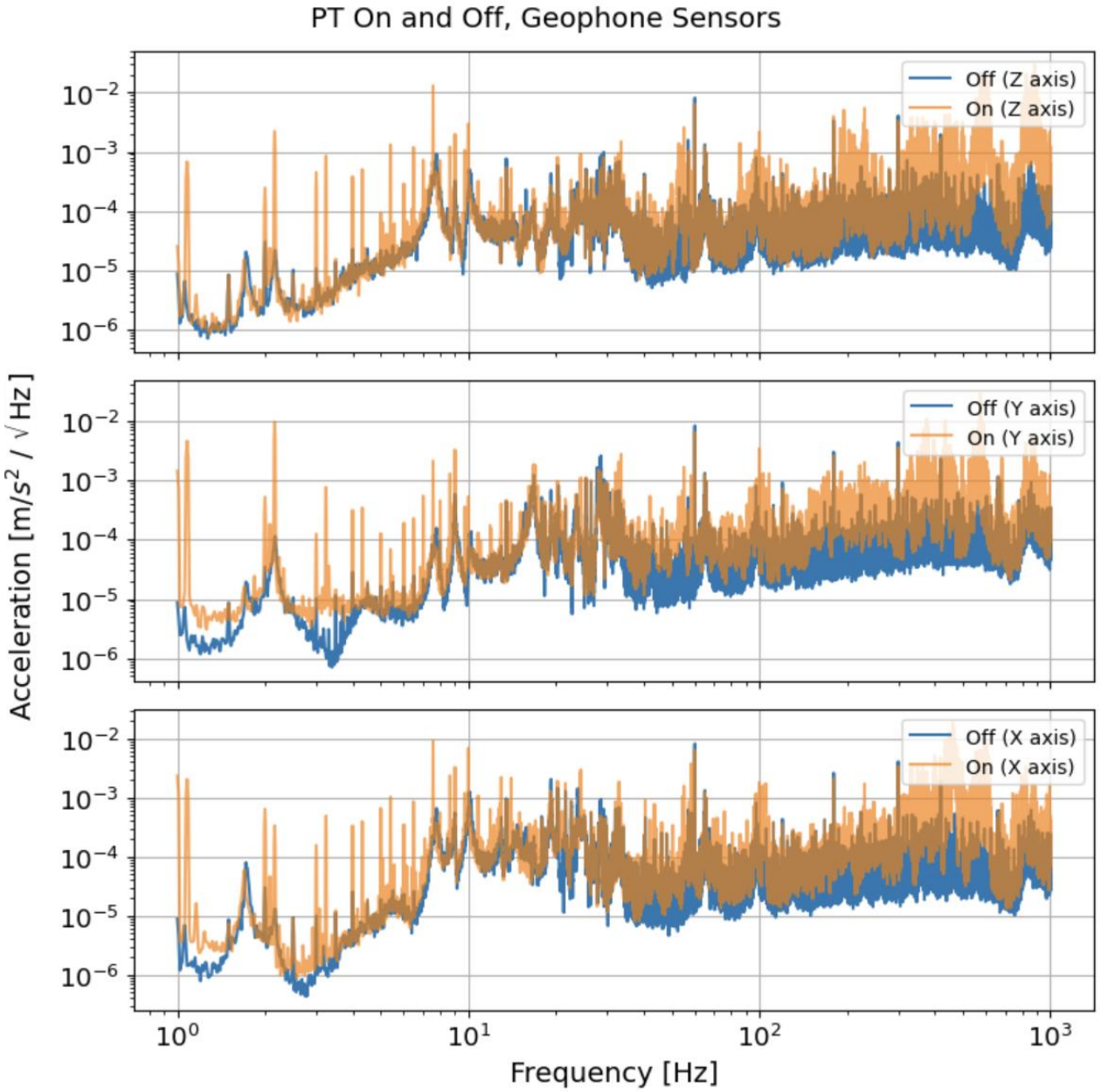
[4] - curie paper / supercdms

[5] E. Olivieri, J. Billard, M. De Jesus, A. Juillard, and A. Leder,"Vibrations on pulse tube based Dry Dilution Refrigerators for low noise measurements" vol. 858, pp. 73-79, Jun. 2017, doi:https://doi.org/10.1016/j.nima.2017.03.045.

[6] PCB Piezotronics, Vibration Fundamentals, https://www.pcb.com/contentstore/mktgcontent/linkeddocuments/Vibration/TM-VIB_PosterBook_Lowres.pdf (accessed Mar. 2, 2026).

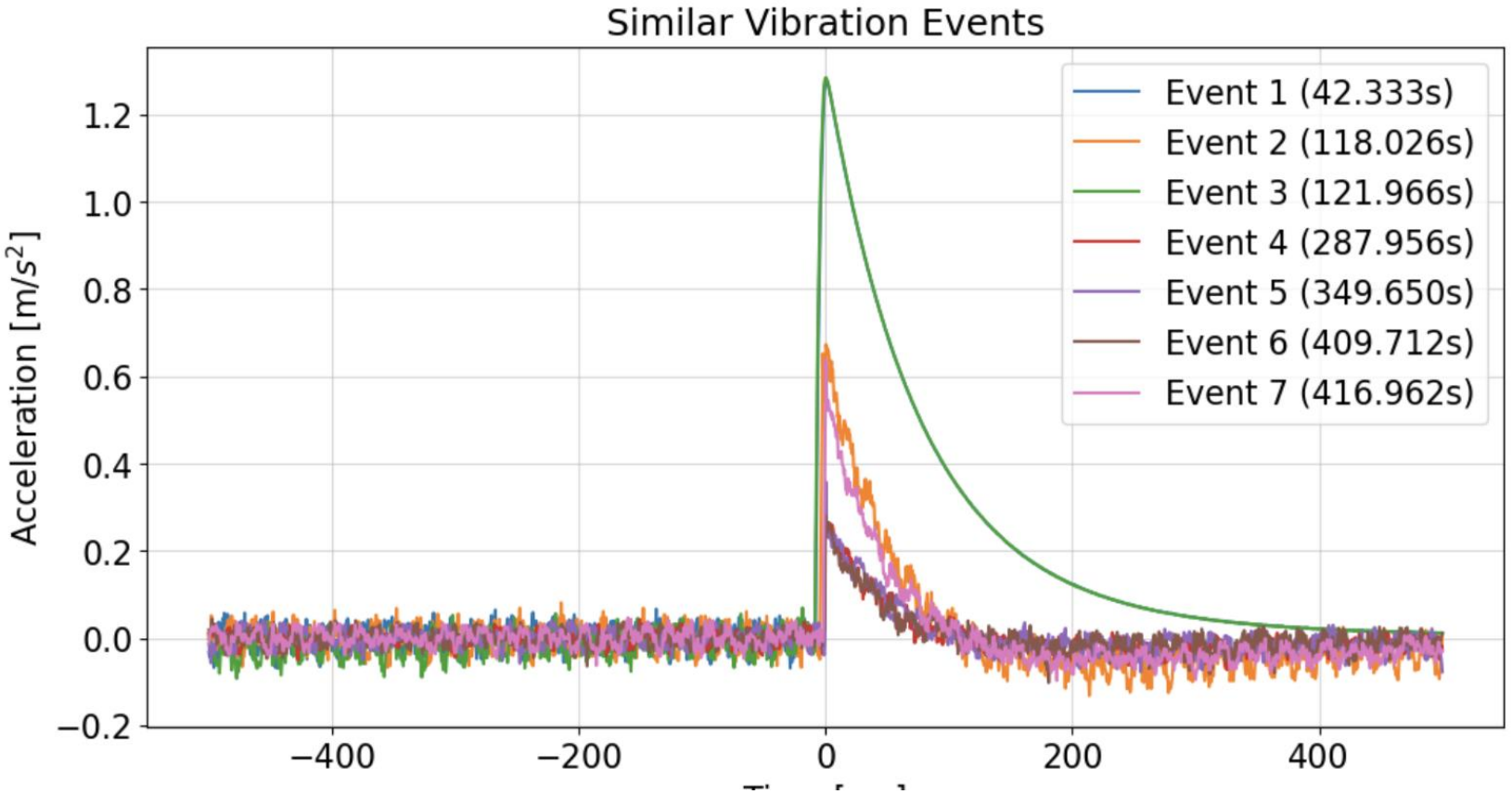
Supplemental slides


PT On and Off
Off (2271A)
On (2271A)
Off (393B05)
On (393B05)
Off (X axis)
On (X axis)
Acceleration [m/s² / √Hz]
Frequency [Hz]


PT On and Off, Geophone Sensors
Off (Z axis)
On (Z axis)
Off (Y axis)
On (Y axis)
Off (X axis)
On (X axis)
Acceleration [m/s² / √Hz]
Frequency [Hz]

2271A Noise

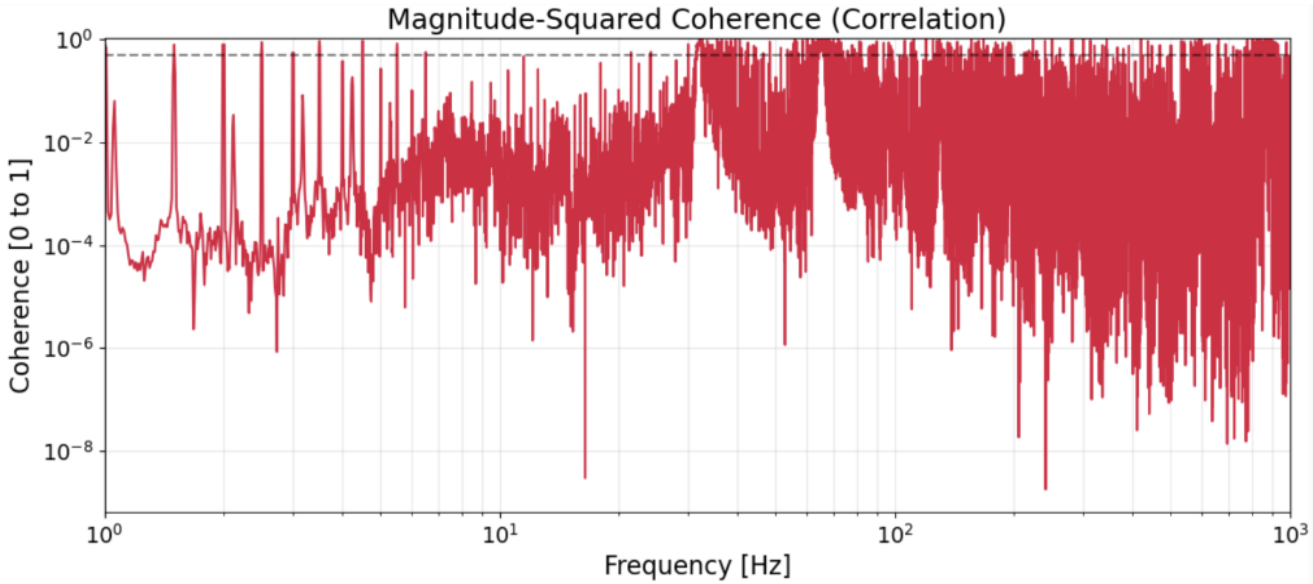
- Strange vibration events, some sort of electrical discharges?



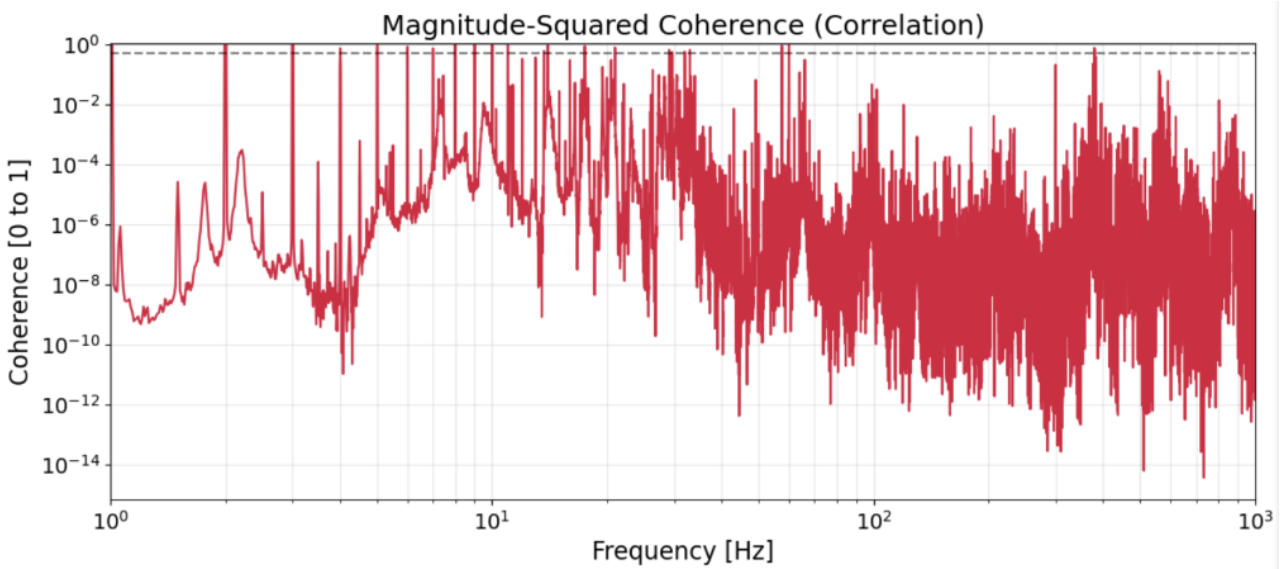
Calculating Coherence between Lowtemp and Geophones

$$C_{i,k} = \frac{|G_{i,k}|^2}{G_{i,i}G_{k,k}}$$

2271A and random geophone:

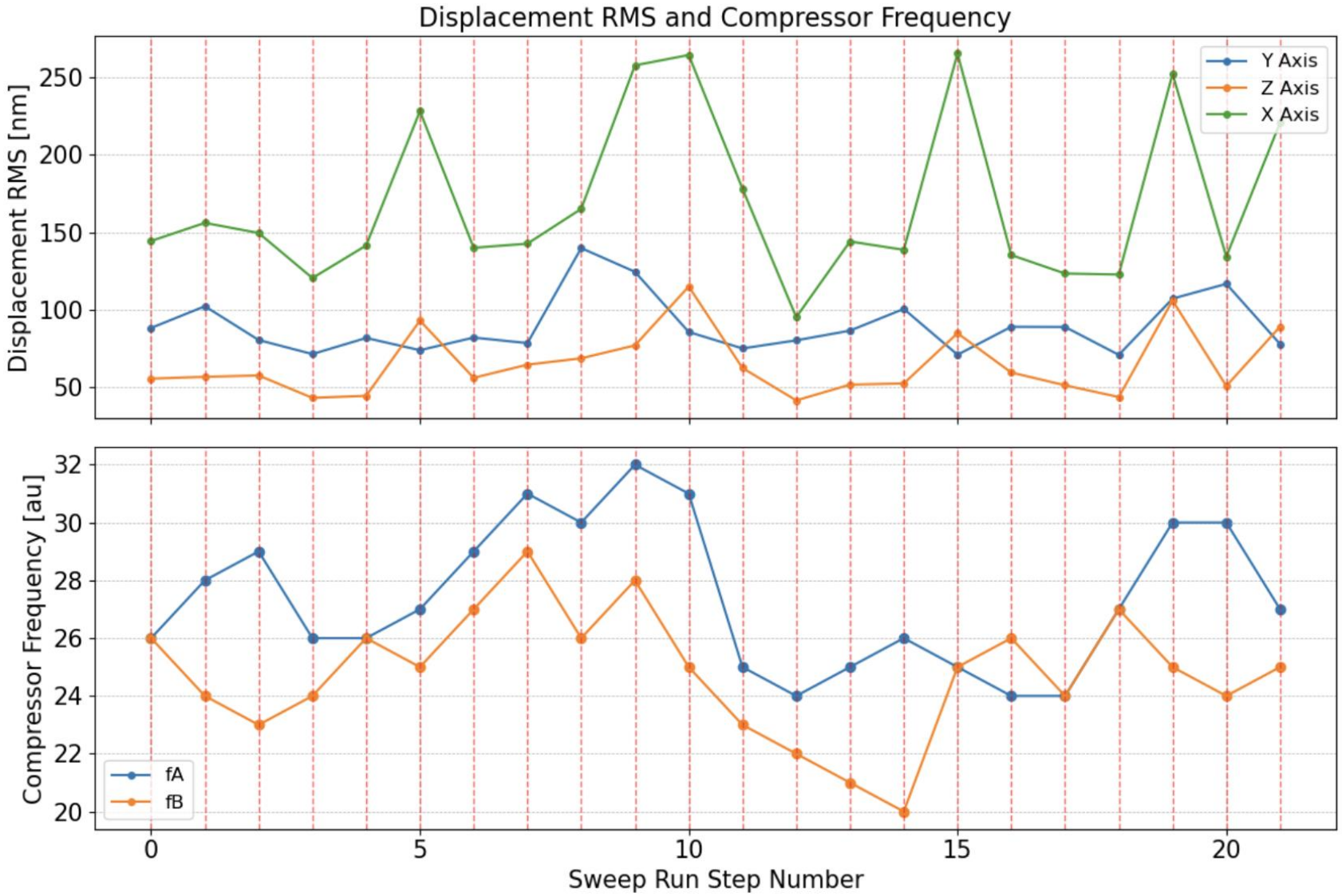


Two random geophones:



Compressor Frequency Sweep

- Measured Displacement RMS for each 10 minute compressor frequency change
- The typical variance in displacement RMS is a +/- 2 nm, so these values should be fairly accurate.

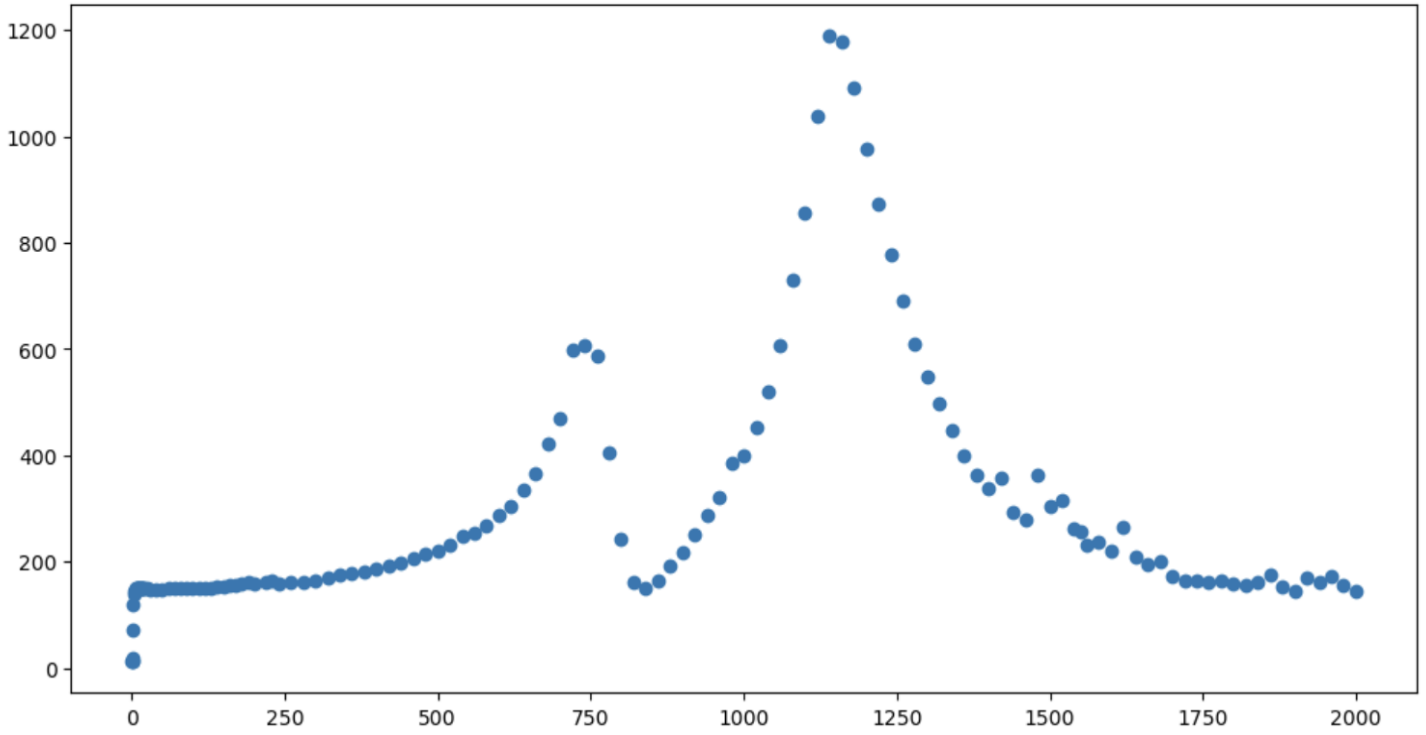


Geophone Analysis

- Numpy.interp function used to create an interpolation for sensitivity (V / m/s) at a given frequency
- Calculated PSD as shown previously, then converting to acceleration PSD

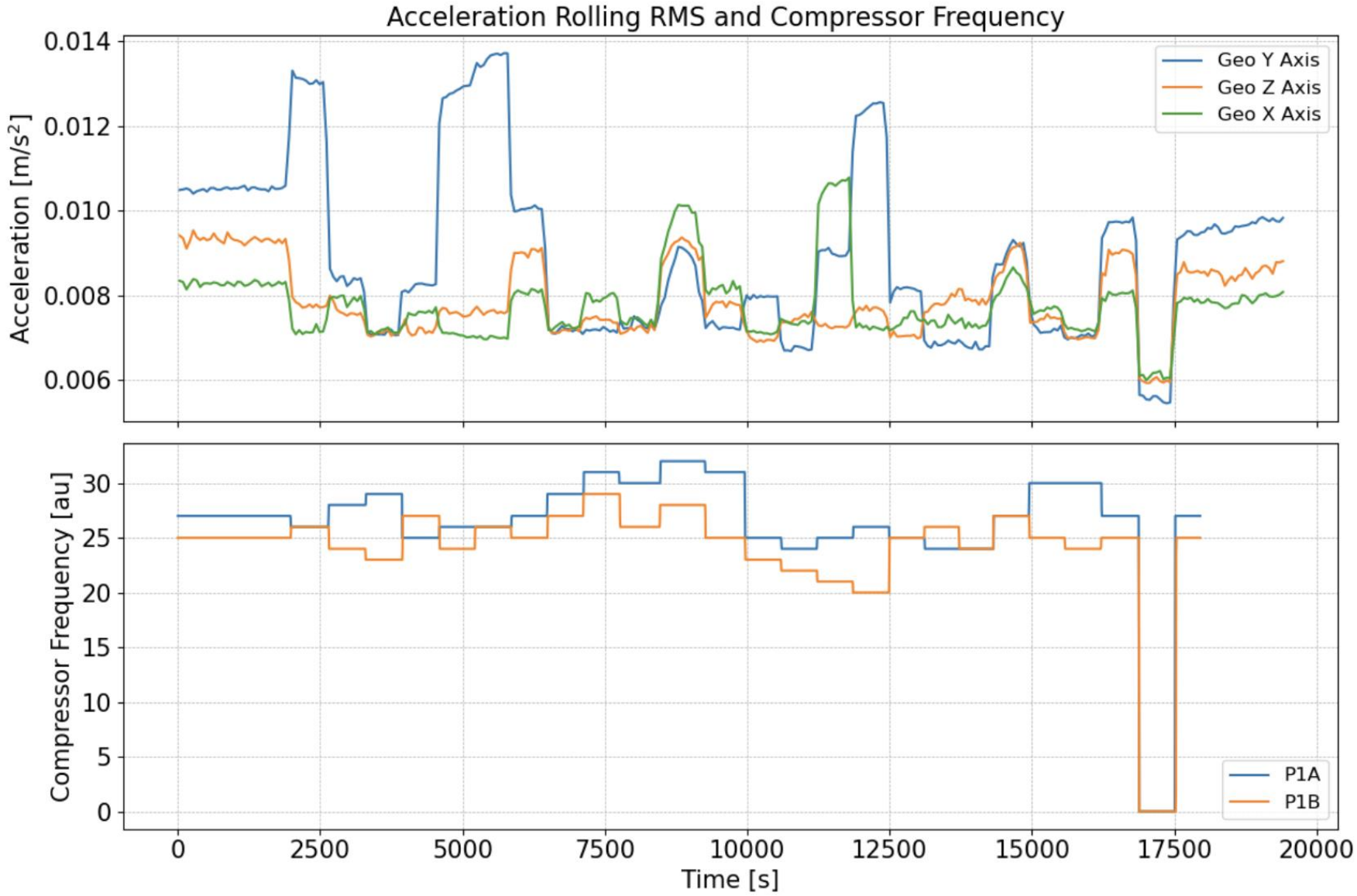
$$PSD_a = (PSD_v)_i(2\pi f_i)/(\text{Sensitivity})$$

sensitivity converts voltage to m/s, and the other term converts velocity PSD to acceleration PSD.



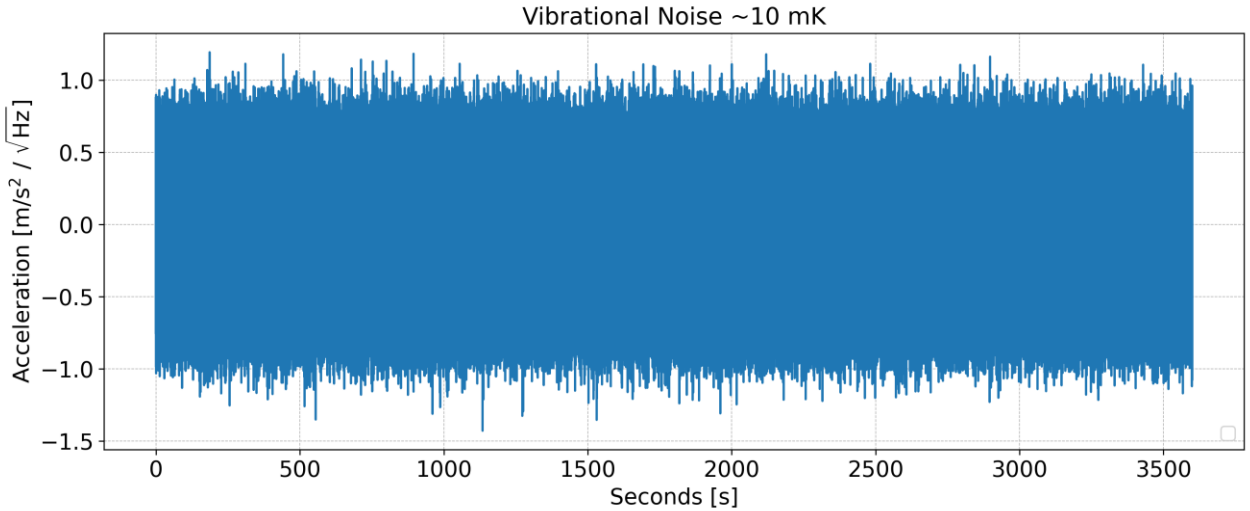
Geophone Calibration Data (V per m/s vs frequency)

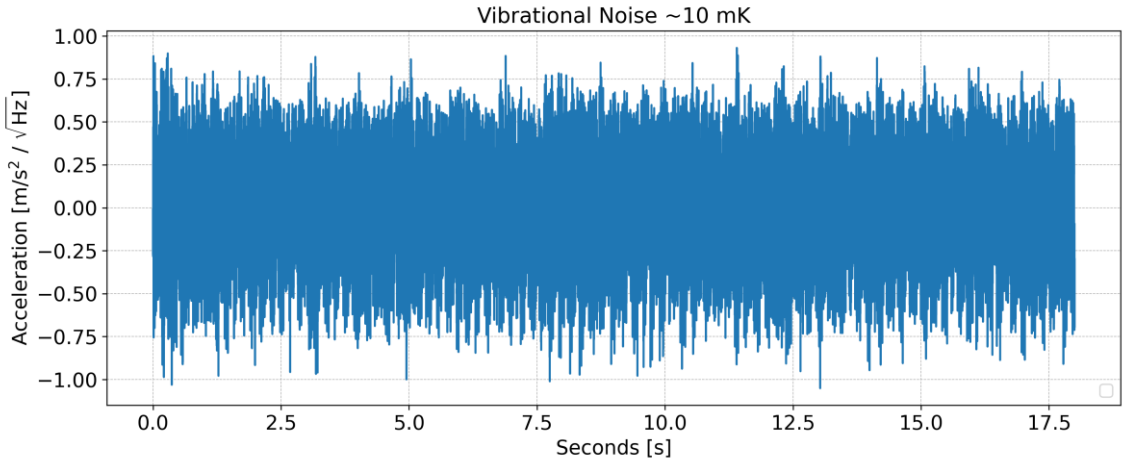
Rolling RMS


Acceleration Rolling RMS and Compressor Frequency
Acceleration [m/s²]
0.014
0.012
0.010
0.008
0.006
Geo Y Axis
Geo Z Axis
Geo X Axis
Compressor Frequency [au]
30
25
20
15
10
5
0
P1A
P1B
0
2500
5000
7500
10000
12500
15000
17500
20000
Time [s]

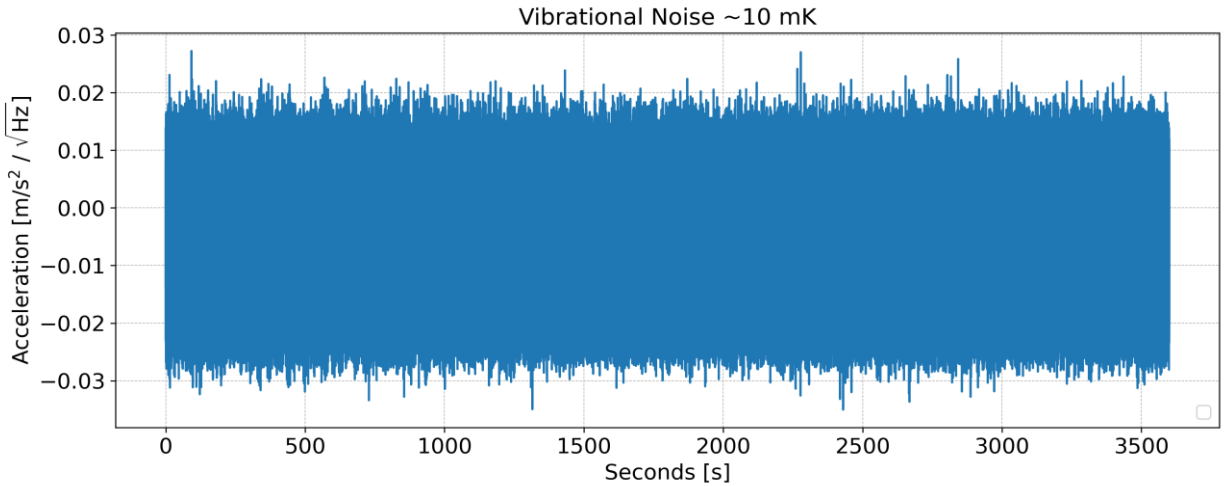
Time Series data

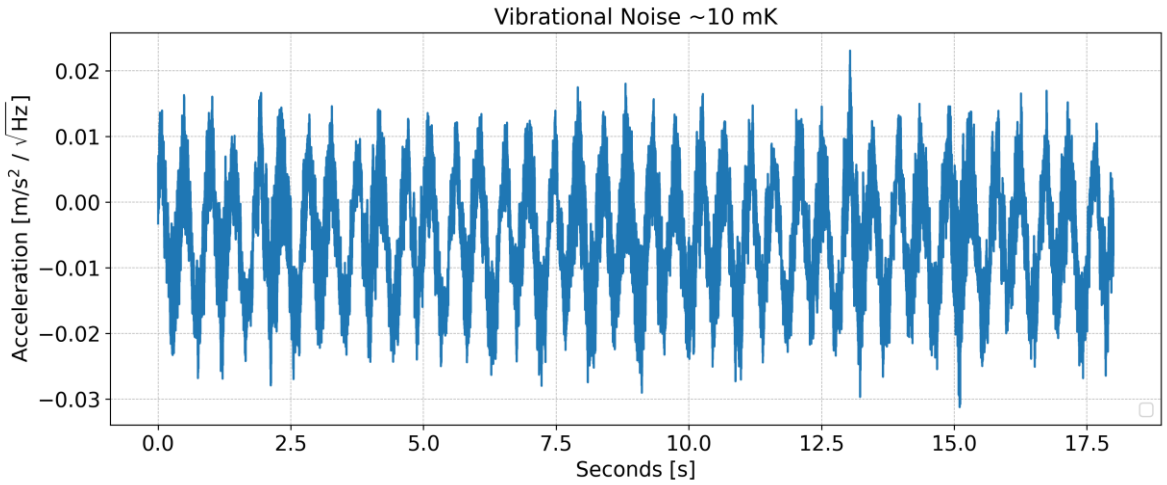
2271A





Geophones





Room Temperature, PT Off

